Odoribacter splanchnicus mitigates *Salmonella*-induced gut inflammation and its associated pathogenesis via its secreted bacteriocin

Dipasree Hajra[1], Debapriya Mukherjee [1], Rhea Vij [1], Raju S Rajmani [2], Venkatareddy Dadireddy[3], Deepakash Das[4], Tanweer Husain[4], Mahipal Ganji[3], Utpal Tatu [3], Chakravortty D [1,5 #]

[1]Department of Microbiology & Cell Biology, Indian Institute of Science

[2]Centre of Infectious Disease Research, Indian Institute of Science, Bangalore, India

[3]Department of Biochemistry, Indian Institute of Science, Bangalore, India

[4]Department of Developmental Biology & Genetics, Indian Institute of Science, Bangalore, India

[5]Adjunct Faculty, School of Biology, Indian Institute of Science Education and Research, Thiruvananthapuram

#Corresponding author: Prof. Dipshikha Chakravortty

Email: dipa@iisc.ac.in

Tel. No. 0091 80 22932842

ABSTRACT

Foodborne pathogens continue to be a leading concern of health hazards worldwide claiming the lives of millions. The emergence of drug-resistant strains poses a great threat to global world health management. Therefore, designing novel therapeutic strategies aiming to overcome pathogen burden is of utmost importance. Here, we identified the crucial role of a gut-commensal species, *Odoribacter splanchnicus* in mitigating *Salmonella* pathogenesis in mice by inhibiting gut vascular barrier disruption, acute inflammatory infection signs, *in vivo* biofilm formation and by preserving tight junction protein functions upon pre-colonization. Further, our *in vitro* studies revealed that not only live *O. splanchnicus* (OS) but also its culture supernatant inhibit *Salmonella* biofilm formation, intracellular proliferation in human intestinal

cells, and its virulence gene expression. In addition, OS's inhibitory effect on *Salmonella* is specific as *Enterococcus faecalis* fails to exert an inhibitory effect on *Salmonella*. Further, our results depicted that the specific protective role of OS acts over a broad spectrum as it confers protection against flagellated Gram-positive, *Listeria monocytogenes* and Gram-negative, *Salmonella* Typhimurium foodborne pathogens, as opposed to non-flagellated *Shigella flexneri*. Moreover, OS conferred protection even after its administration to mice post-establishment of infection highlighting its therapeutic potential. Using several biochemical and proteomics approaches, we characterized the key active molecule secreted by OS to limit intracellular *Salmonella* and *Listeria* replication in human intestinal epithelial cells by regulating key virulence effectors and flagella. Collectively, our study highlights the broad-spectrum protective role of OS in mitigating *Salmonella* and *Listeria* pathogenesis and implicates its therapeutic potential.

Keywords: *Salmonella* pathogenesis, **Gut vascular barrier permeability**, **inflammation**, **inter-species bacterial regulation**, ***Listeria***, ***Odoribacter splanchnicus***, **gut commensal**, **biofilm, flagella**

INTRODUCTION

The existence of the gut vascular barrier (GVB) acts as a protective barrier against the entry of microorganisms into systemic blood circulation(1, 2). Enteric pathogens such as *Salmonella enterica* can cross the mucus and intestinal epithelial barrier, ultimately leading to GVB damage and systemic dissemination(1). The gut microbiota plays another major role in the maintenance of the intestinal epithelial barrier by the production of several metabolites such as Short-chain fatty acids (SCFAs), indoles, and polyphenol metabolites that contribute to epithelial barrier integrity and turnover by regulating the expression of Tight-junction (TJ) genes(3). Additionally, these SCFAs have the potential to exert anti-inflammatory properties by regulating cytokine production, mucosal immune cell migration, and secretion of

antimicrobial peptides (AMPs) by intestinal epithelial cells and macrophages(4, 5). Our previous study reported an incidence of increased *Salmonella* dissemination in blood, liver, and spleen upon SIRT1 and SIRT3 inhibition owing to the increased inflammatory response(6).

Salmonella gains entry inside the body through the orofecal route along with the ingestion of contaminated food and water. *Salmonella* resist the low acidic pH of the stomach by utilizing the acid tolerance response (ATR) genes and finally reach the lumen of the small intestine(7). In the intestinal tract, it uses specialised microfold (M) cells for macro-pinocytic entry. The pathogen gains entry into the non-phagocytic epithelial cells via its *Salmonella* Pathogenicity Island-1 (SPI-1) effectors to breach the intestinal barrier (8). Once traversing through the mucosal lining of the gut epithelium, it reaches the lamina propria (8). Apart from M cells, the dendritic cells can also sample the bacteria from the lumen to the lamina propria. In the lamina propria, it encounters various host immune cells like neutrophils, macrophages, dendritic cells and so on. Macrophages, dendritic cells, and neutrophils are responsible for successful dissemination throughout the body through the reticulo-endothelial system (RES) to the secondary organs such as Mesenteric Lymph Node (MLN), liver and spleen(8). *Salmonella* relies on the SPI-2 secretion for its intracellular and intravacuolar life by injecting various virulence factors into the host cell cytosol (9).

Here, in this present study, we aimed to understand this exact mechanism of *Salmonella* dissemination and whether colonization with a gut commensal like *Odoribacter splanchnicus* (OS) could ameliorate the *Salmonella*-induced inflammation and in turn its pathogenic dissemination. OS, belonging to the order Bacteroidales, is a common, member of the human intestinal microbiota. A decrease in *Odoribacter* abundance has been linked to different microbiota-associated diseases, such as non-alcoholic fatty liver disease, cystic fibrosis and inflammatory bowel disease (IBD)(10). A recent report indicated the ability of OS and its effectors transported in Outer membrane vesicles (OMVs) to exhibit anti-inflammatory effects

79 on the gut epithelium(10). Further, OS has been implicated to confer resistance against colitis
80 and colorectal cancer(11).

81 Our study shows that OS colonization reduces *Salmonella* gut colonization, its organ load, and
82 its systemic dissemination even under aggravated inflammatory responses such as SIRT1 or
83 SIRT3-inhibited condition. OS ameliorates acute *Salmonella*-induced inflammation and its
84 associated pathogenesis by inhibiting GVB damage and preserving tight junction protein
85 functions. Further, we demonstrate that not only live OS but also its culture supernatant inhibits
86 *Salmonella in vitro* biofilm formation, intracellular proliferation in human intestinal cells, and
87 its virulence gene expression. Subsequently, our results depict that the specific protective role
88 of OS acts over a broad spectrum as it confers protection against both flagellated Gram-
89 positive, *Listeria monocytogenes* and Gram-negative, *Salmonella* Typhimurium foodborne
90 pathogens in contrast to non-flagellated *Shigella flexneri*. Furthermore, OS conferred
91 protection even after its administration to mice post-establishment of infection highlighting its
92 therapeutic potential. Subsequently, we identified the key OS-secreted bacteriocin protein
93 responsible for limiting intracellular *Salmonella* and *Listeria* replication in human intestinal
94 epithelial cells by regulating virulence genes such as flagella. Overall, our study implicates the
95 broad-spectrum protective role of OS in mitigating foodborne infections caused by *Salmonella*
96 and *Listeria* pathogenesis.

97 **RESULTS**

98 ***O. splanchnicus* hinders *Salmonella* colonization in mouse gut and its systemic**
99 **dissemination**

100 To denote the role of OS in governing *Salmonella* pathogenesis, we colonized C57BL/6 mice
101 with 10^5 CFU of OS 1 day prior to *Salmonella* infection via the oral route and validated the
102 colonization by undertaking OS 16S rRNA qPCR analysis (Fig 1, A-B). OS pre-colonized mice

103 showed decreased susceptibility to *Salmonella* infection in comparison to the non-colonized
104 mice cohort which succumbed to death by day 7 post-infection (p.i.). Contrastingly, 100% of
105 the OS colonized mice were alive even at day 8 post *Salmonella* infection (Fig 1, C). OS non-
106 colonized mice exhibited increased weight loss percentage upon *Salmonella* infection and OS
107 pre-colonization led to diminished weight reduction percentage (Fig 1, D). The increased
108 *Salmonella* organ loads and bacterial dissemination in the non-colonized mice groups were
109 reversed upon OS colonization (Fig 1, E-F). Our previous findings revealed increased bacterial
110 dissemination owing to heightened inflammatory responses in the case of SIRT1 and SIRT3
111 knockdown or inhibitor-treated conditions(6). Therefore, in this study, we intended to examine
112 whether OS could exert its protective role against *Salmonella* infection even in the case of
113 aggravated inflammatory conditions such as in the case of SIRT1 or SIRT3 inhibited
114 conditions. Our result suggests that even in aggravated conditions of inflammation and
115 *Salmonella* dissemination under SIRT1 or SIRT3 inhibitory conditions, OS could prevent
116 *Salmonella* colonization and its dissemination (Fig 1,D-G).

117 ***O. splanchnicus* colonization ameliorate the acute *Salmonella-induced* inflammation and**
118 **its associated pathogenesis**

119 Heightened inflammatory responses facilitate *Salmonella* dissemination in mice(6). Thus, we
120 hypothesized that OS gut colonization might ameliorate the *Salmonella*-induced inflammation.
121 ELISA-mediated IL-6 serum quantification revealed reduced IL-6 production upon *S.*
122 Typhimurium (STM) infection in the OS colonized mice group to the non-colonized cohort
123 (Fig 2, A). The reduced IL-6 production upon OS colonization was even observed in elevated
124 inflammatory conditions of SIRT1 or SIRT3 inhibition. To combat the enteric pathogen
125 challenge, the host employs one of its major defence arsenals, that is, the production of
126 antimicrobial peptides (AMPs)(12, 13). STM infection induces enhanced mRNA expression of
127 AMPs in mice with respect to the uninfected control. We found that OS colonization in mice

128 resulted in the downregulation of several AMP genes such as Lysozyme-C1 precursor,
129 Angiogenin-4 precursor, CCL20, Beta-defensin-4 and Regenerating-islet-derived 3 beta-
130 precursor (Fig 2, B). Mucus lining serves as another crucial barrier against the entry of enteric
131 pathogens. However, enteric pathogens adopt several strategies to circumvent this barrier to
132 reach the underlying epithelium. To assess the mucin layer dynamics upon the *Salmonella*
133 challenge, we assessed MUC2 expression in the ileal tissues of OS colonized versus non-
134 colonized mice groups. Our result depicted enriched MUC2 expression in the OS non-
135 colonized mice cohort compared to the colonized cohort (Fig.2, C). The increase in the mucus
136 lining upon *Salmonella* infection could be one of the host defense mechanisms to bolster the
137 barrier and exclude pathogens(14). As per previous literature, the rate of mucin production is
138 modulated by several stimuli including inflammatory cytokines (15), vasoactive antimicrobial
139 peptides, and other innate and adaptive immune responses (16). Germ-free mice depict a
140 reduced number of goblet cells, and mucin storage granules(17) as well as reduced expression
141 of AMPs(18). The haematoxylin eosin-stained intestinal sections suggested increased intestinal
142 tissue damage with irregularly organized villi, necrotic submucosa layer, and detached
143 intestinal cells in all the STM-infected non-OS-colonized cohorts. However, OS pre-
144 colonization restored the intestinal tissue architecture in all the mice cohorts (Fig 2, D).

145 ***O. splanchnicus* restricts *Salmonella*-mediated GVB damage by promoting tight junction**
146 **gene expression**

147 *Salmonella* enters the intestinal epithelial milieu by breaching the gut vascular barrier (GVB)
148 and by inducing tight junction disruption. Upon ingestion, *Salmonella* like other food-borne
149 antigens enters into the Mesenteric Lymph Node (MLN) by accessing the lymphatics and
150 subsequently gains entry into the liver via the bloodstream(19). The translocation of the
151 pathogen across the blood endothelial cells is governed by the integrity of the GVB(1). The
152 GVB architecture is maintained by several tight junction and adherens junction proteins that

153 control paracellular trafficking(20, 21). PV-1 (plasmalemma-vesicle associated protein-1)
154 expression is a determinant of GVB damage and heightened PV-1 expression denotes EC
155 permeability(22, 23). Our data depict heightened PV-1 marker expression alongside reduced
156 tight junction protein mRNA expression such as *Tjp1* and *Claudin5* upon *Salmonella* infection
157 correlating with increased bacterial dissemination in blood and liver (Fig. 3, A-B, Fig. S1, A).
158 CD34, an endothelial marker lining the blood vessels (24, 25), has been promoted upon OS
159 colonization in *Salmonella*-infected mice intestines indicative of intact vasculature (Fig. 3, B-
160 D, Fig.S1, B). On the contrary, OS mice cohorts exhibited reduced CD34 expression in
161 secondary sites of dissemination such as the liver, suggesting toward reduced vasculature
162 (Fig.S1, C). Therefore, OS pre-colonization attenuates the *Salmonella* dissemination by
163 exhibiting reduced PV-1 protein expression and promoting tight junction protein expression
164 (Fig. 3, A-D). Angiogenesis is one of the processes that facilitate bacterial dissemination.
165 Previous studies in *Mycobacterium marinum* have shown that transcriptional induction of pro-
166 angiogenic markers like *Vegfa* contributes to increased bacterial burden and dissemination(26).
167 In our study, OS pre-colonization in the gut resulted in reduced expression of the pro-
168 angiogenic *Vegfa* in the infected liver tissues, which coincided with the reduced *S.*
169 Typhimurium burden in the bloodstream and liver (Fig S1, D). Together, our results depict the
170 ability of OS to suppress angiogenesis and in turn STM dissemination. OS could exert its
171 angiogenesis inhibitory effects even in instances of aggravated dissemination conditions like
172 in the case of SIRT1 and SIRT3 inhibitor treatment in mice. Previous literature suggested
173 reduced expression of *Axin2,* a β catenin target gene, upon wildtype *Salmonella* infection, even
174 after Wnt3a stimulation suggesting that *Salmonella* affects the GVB by inhibiting canonical
175 Wnt signalling (1). Here, our results suggest that OS pre-colonization restores the *Salmonella*-
176 triggered attenuated Wnt signalling response with increased Axin2 expression in the
177 *Salmonella*-infected intestinal and thereby restricts GVB damage and dissemination (Fig. S1,

178 E). The integrity of the infected mice gut was estimated by the gut permeability assay using
179 FITC-Dextran. Our results indicate increased gut vascular permeability upon *Salmonella*
180 challenge which declined upon OS pre-colonisation.

181 ***O. splanchnicus* culture supernatant restricts *Salmonella* biofilm formation and**
182 **intracellular proliferation in human intestinal cells**

183 To delineate the mechanism behind the protective role of OS against *Salmonella* pathogenesis,
184 we performed *Salmonella* infection studies in human intestinal epithelial cell line Caco-2 in
185 the presence of OS. The intracellular survival assay suggested decreased STM invasion and
186 subsequently attenuated intracellular replication within the infected Caco-2 cells upon co-
187 infection with live OS and in the presence of OS culture supernatant (Fig 4, A-B). However,
188 STM co-infection with fixed OS showed percent invasion and intracellular replication like that
189 of STM infection (Fig 4.5, A-B). Together, these results hinted at the presence of some secreted
190 inhibitory components in the OS culture supernatant that has the propensity to limit STM
191 infection. The reduced inhibition and proliferation of STM within Caco-2 cells in presence of
192 OS was subsequently validated in immunofluorescence studies, wherein STM showed a
193 significant reduction in invasion at 2hr p.i. and intracellular proliferation at 16hr p.i. in case of
194 OS co-infection (Fig 4, C-D). Similar results were obtained upon infection with the human-
195 restricted serovar *S.* Typhi (STY) to the Caco-2 cells wherein OS and its supernatant attenuated
196 STY invasion and intracellular replication (Fig. 4, E-F). Further, we assessed the *in vitro* growth
197 of the STM in co-culture conditions with OS or in the presence of OS culture supernatant in
198 anaerobic conditions to mimic the microaerophilic or hypoxic environment of the gut or in
199 aerobic culture conditions. We observed no significant delay *in vitro* growth of STM at its
200 initial lag to log phase of its growth in the presence of OS supernatant or with live OS under
201 anaerobic culture conditions (Fig S2, A-B). In aerobic growth conditions as well, *Salmonella*
202 growth remained unperturbed even in the presence of OS or its culture supernatant (Fig S2, C-

203 D). Several previous studies have corroborated the ability of commensal bacterial culture
204 supernatants to inhibit colonization and the biofilm formation of several pathogens. For
205 instance, a commensal bacterium, *Staphylococcus epidermis*, could inhibit biofilm formation
206 and nasal colonization of its pathogenic counterpart, *Staphylococcus aureus* (27). Moreover,
207 biofilm formation is also regulated at the interspecies level. Indole is an inter-species biofilm
208 regulator wherein it decreases *E. coli* biofilm formation and facilitates biofilm formation of
209 pseudomonads (28). STM form biofilm to colonize host, evade host defence arsenals and
210 antibiotics, persist in case of chronic infections, and transmit to new hosts (29, 30). We,
211 therefore, examined the biofilm formation of STM in presence or absence of live, PFA-fixed-
212 OS or OS culture supernatant. STM exhibited biofilm formation defect, in the presence of live
213 OS or OS supernatant (Fig 4, G). However, the STM biofilm inhibitory property of STM was
214 diminished upon treatment with paraformaldehyde (PFA)-fixed OS (Fig 4.5, G). Further,
215 qPCR-mediated gene expression studies of *Salmonella* biofilm genes revealed decreased
216 expression of genes regulating biofilm (*csgD*, *csgA*, *bapA*) under treatment with live OS or its
217 culture supernatant (Fig.4, H-J). Flagella-mediated attachment and several virulence factors
218 such as SPI-1 and SPI-2 genes are responsible for *Salmonella* pathogenesis and its biofilm
219 formation (31-33). Therefore, we evaluated a few of the *Salmonella* flagellar and SPI-1 and
220 SPI-2 gene expression in the presence or absence of OS or its culture supernatant via
221 quantitative real-time PCR. Our results depicted attenuated expression of flagellar gene (*fliC*),
222 SPI-1 (*sipC*) and SPI-2 (*pipB2*) genes both in the presence of live OS and its spent media but
223 not in presence of PFA fixed-OS (Fig. 4, K-M). The loss in *Salmonella* flagellar motility was
224 further validated via TEM imaging wherein OS or its supernatant reduced the flagella
225 formation of *Salmonella* considerably (Fig.4, N). Together, our results implicate the ability of
226 OS to inhibit STM biofilm formation via active secretion of certain inhibitory molecules in the
227 supernatant.

228 ***O. splanchnicus* inhibitory effect on *Salmonella* is specific as *Enterococcus faecalis*,**
229 **another gut resident microbe, fail to inhibit *Salmonella* intracellular proliferation or**
230 **biofilm formation**

231 The resident gut microbes provide colonization resistance against invading pathogens by
232 deploying several mechanisms, including the production of inhibitory molecules, nutrient
233 competition, maintenance of the intestinal epithelial integrity, immune activation, and via the
234 deployment of bacteriophages (34, 35). To understand whether our observed inhibitory trait of
235 OS against *Salmonella* is due to a common colonization restriction phenomenon of gut
236 microbes via competitive inhibition, or it is a specific phenomenon, we evaluated the role of
237 another gut resident microbe, *Enterococcus faecalis* on *Salmonella* intracellular replication in
238 human intestinal epithelial cells and *Salmonella* biofilm formation. *Enterococcus sp.* belong to
239 the phylum of Firmicutes in the family Enterococcaceae. Approximately, 10^6-10^7 *Enterococcus*
240 *sp*. reside in the human intestine with major abundance of *E. faecalis* (10^5-10^7 CFU/gm faeces)
241 and *E. faecium* (10^4-10^5/gm faeces) (36). *E. faecalis*, *E. faecium*, *Bifidobacterium sp*.
242 *Lactobacillus sp.,* and *E. coli* colonize the gut of healthy breastfed infants during the initial 7-
243 10 days post birth (37). Our intracellular survival assay data showed no defect in *Salmonella*
244 invasion or intracellular replication capability in Caco-2 cells in presence or absence of *E.*
245 *faecalis*, its culture supernatant or PFA-fixed *E. faecalis* (Fig. 5, A-B). Moreover, *E. faecalis*
246 or its *E. faecalis* supernatant did not inhibit *Salmonella* biofilm formation (Fig. 5, C). Together,
247 our results suggest the inability of *E. faecalis* to inhibit *Salmonella* invasion, intracellular
248 proliferation or its *in vitro* biofilm formation, thereby highlighting the specificity of OS in
249 restricting *Salmonella* pathogenesis.

250 ***O. splanchnicus* confers protection against another foodborne pathogen *Listeria***
251 ***monocytogenes* but not against *Shigella flexneri***

252 To understand whether OS exerts a common broad-spectrum protection or colonization
253 resistance against other foodborne pathogens such as *Listeria monocytogenes* or *Shigella*
254 *flexneri*, we orally infected 6-8-week-old C57Bl/6 mice with 10^8 or 10^7 CFU of *L.*
255 *monocytogenes* (LM) or *S. flexneri* (SF), respectively 1 day post colonization with 10^5 CFU of
256 *O. splanchnicus* for organ burden evaluation. For survival study, mice were orally gavaged
257 with 10^9 or 10^8 CFU of *L. monocytogenes* or *S. flexneri,* respectively. OS-colonized mice
258 exhibited increased survival rates upon LM challenge in comparison to the non-colonized mice
259 cohort (Fig. 6,A). Contrastingly, both OS-colonized and non-colonized mice showed
260 comparable survival upon SF challenge (Fig. 6, G). In line with the survival data, increased
261 bacterial burden was observed in blood, MLN, spleen and liver alongside enhanced percent
262 loss in mice body weight, increased GVB damage, mucin and AMPs production in the case of
263 *Listeria* infection in non-colonized mice group with respect to OS-precolonized- mice group
264 (Fig. 6, B-F). Conversely, *Shigella* infection resulted in comparable organ loads and
265 comparable signs of pathogenesis in both cohorts (Fig. 6, H-L). In a similar line to *Salmonella*
266 infection, OS mitigated host antimicrobial response with reduced expression of antimicrobial
267 peptide transcripts and Muc2 production during LM infection as opposed to SF infection
268 amounting to reduced intestinal tissue damage. Further, OS promoted tight junction functions
269 during *Listeria* infection with reduced GVB damage and *Vegf* expression unlike during *Shigella*
270 challenge (Fig. S3, A-J). Moreover, OS colonization could restrict the *in vivo Salmonella* and
271 *Listeria* biofilm within the spleens of the infected mice cohorts as opposed to the non-colonized
272 mice cohorts (Fig.S3, K-L). The contrasting results between *Listeria* and *Shigella* could be
273 attributed to the presence of flagella in both *Salmonella* and *Listeria* but not in *Shigella*. Like
274 *Salmonella*, *in vitro* culture of *Listeria* with OS or its culture supernatant led to a loss in flagella
275 as evidenced via the TEM imaging (Fig.S3, M). Since flagella is one of the factors facilitating
276 biofilm formation and invasion, OS could inhibit both *Salmonella* and *Listeria* colonisation

277 and biofilm formation. Similar to *Salmonella* infection, OS colonization enhanced CD34
278 expression in *Listeria*-infected mice intestines and reduced CD34 expression in the *Listeria*-
279 infected liver (Fig. S3 N-O). Further, LM exhibited attenuated intracellular proliferation within
280 human intestinal Caco-2 cells upon live OS or OS supernatant treatment (Fig. S4). Altogether,
281 this result hints at the potency of OS to act broadly against Gram-positive and Gram-negative
282 bacteria and probably via regulation of flagella formation.

283 **The protective role of *O. splanchnicus* against *Salmonella* Typhimurium and *Listeria***
284 ***monocytogenes* persists even on administration post-establishment of infection**

285 Next, we sought to examine whether the protective role of OS against *Salmonella* and *Listeria*
286 is sustained when the infection has been fully developed and whether it can serve as a treatment
287 regimen against foodborne diseases. Our results indicate the protective ability of OS against
288 both foodborne pathogens in their intestinal phase of infection when administered at 1-day
289 post-infection (dpi) as depicted by lower pathogen loads in all the organs and blood along with
290 reduced percent weight loss at 5th-day post-*Salmonella* or *Listeria* challenge in the OS-
291 administered (1-dpi) cohort when compared to the untreated cohorts (Fig. 7,A-K). Although
292 the protective ability of OS persists even upon establishment of infection when administered
293 at 3rd-day post-*Salmonella* or *Listeria* challenge as indicated by reduced organ loads and
294 percent weight loss in the OS-colonized cohorts, the extent of protection is lower compared to
295 its administration at 1-dpi (Fig. 7, L-W), Further, the OS challenge at 1-dpi reduced the mice's
296 susceptibility to the *Salmonella* and *Listeria* challenge(Fig. 7, L,R). However, administration
297 of OS at 3-dpi delayed the death of the *Salmonella* and *Listeria*-infected mice cohorts by 1 day
298 (Fig. 7, L,R). In line with the survival and organ burden data, OS treatment at both 1st and 3rd
299 dpi reduced both *Salmonella* and *Listeria*-induced GVB damage with reduced PV-1 expression,
300 mucin, AMPs, and *Vegf* expression, alongside promoting tight junction protein (*Tjp1* and
301 *Claudin5*) and *Axin2* expression (Fig. S5A-N). However, OS administration at 3-dpi conferred

302 less protection than at 1-dpi as indicated by the protein expression profiles of Muc2, PV-1, and
303 tight junction protein ZO-1 (Fig. S5, O-P). Moreover, the hematoxylin- eosin-stained intestinal
304 sections revealed reduced intestinal tissue damage with restoration in the villi architecture in
305 the 1- and 3-dpi OS-administered mice cohorts compared to the non-OS-treated groups (Fig.7,
306 X).

307 Moreover, OS colonization could restrict the *in vivo Salmonella* and *Listeria* biofilm within the
308 spleens of the infected mice cohorts as opposed to the non-colonized mice cohorts both when
309 administered at 1-day and 3-day post-pathogen challenge. (Fig.7, Y-Z). Additionally, OS
310 colonization mitigated gut vascular permeability during *Salmonella* and *Listeria* challenges as
311 indicated by reduced FITC-dextran fluorescence units in the plasma both upon pre or post-OS
312 colonization.

313 Furthermore, OS alleviated *Salmonella*-induced intestinal inflammation with reduced IL-1β
314 production in the infected intestinal tissues both upon pre-colonization and post-colonization
315 at 1-dpi (Fig. S6).

316 **Characterization of the inhibitory active molecule within *O. splanchnicus* culture**
317 **supernatant**

318 Our results suggested that not only live OS but also its spent culture supernatant could inhibit
319 *Salmonella* invasion and intracellular proliferation in intestinal human epithelial cells.
320 Moreover, the OS and its supernatant could inhibit STM biofilm formation *in vitro.* This
321 inhibitory effect disappeared upon co-culture with paraformaldehyde-fixed-OS indicating the
322 presumable role of certain inhibitory microbial products secreted by metabolically live OS. To
323 delineate the nature of the secreted molecule/s, we subjected the supernatant to various
324 conditions such as high temperature, divalent cationic chelator, EDTA, and protease (proteinase
325 K), and subsequently assessed the biofilm formation (Fig. S7, A-C). Our biofilm assay

326 suggested that the active molecule is resistant to EDTA treatment and is stable at higher
327 temperatures (Fig. S7, A-B). Nevertheless, the active molecules within the fraction were
328 sensitive to the proteinase K treatment, suggesting the possibility of being protein in nature
329 (Fig. S7, C). SDS-PAGE of the OS supernatant revealed the size of the differential proteins
330 with respect to the media control ranged below 65kDa. (Fig. S7, D). Concentration-dependent
331 estimation of the biofilm activity of the supernatant revealed that the active molecules retain
332 their activity at a minimal concentration of 0.4% v/v (Fig. S7, E). We further fractionated the
333 supernatant using an Amicon 3k MWCO and 10k MWCO ultra filter device (Fig. S7, F-G). We
334 found that the active molecule/s is/ are higher than 3kDa cut-off range eliminating the role of
335 small molecules and ions (Fig. S7, F-G). A summary of the conditions tested for active
336 molecule characterisation and their effective outcome has been summarized in Fig. S7, H.
337 Subsequently, we subjected the culture supernatant to gel filtration chromatography (Fig. S7,
338 I). Out of all the fractions tested, around 24 fractions showed a biofilm inhibitory role. These
339 24 fractions were further subjected to a titration experiment to zero down upon the three
340 fractions with the highest inhibitory activity (A82,A83,A84) (S7, J-L). The gel filtration
341 standard curve run suggested that the active molecules fall in the size range of <60kDa and
342 >3kDa (Fig. S7, I). These three fractions along with the total concentrated supernatant (serving
343 as positive control) and fractions with no or least inhibitory activity (serving as negative
344 control-A31,B12) were ultimately subjected to Reverse Phase LC-MS mass spectrometry.
345 Upon analysis of the proteomics dataset (Fig. S7, M), we obtained 364 proteins showing
346 enrichment in the positive fractions. Among the 364 proteins, 74 proteins exhibited known or
347 predicted function as per UniProt and STRING database and 11 proteins were linked to
348 antibacterial, bacteriostatic, flagella, and biofilm regulation based on data curation and
349 literature survey (Table-S1). We selected bacteriocin proteins exhibiting direct association with
350 antibacterial activity for further analysis. These proteins include bacteriocins which are

351 antimicrobial peptides that can kill or inhibit closely related or unrelated bacterial strains(38,
352 39).

353 ***O. splanchnicus*-derived purified peptide, bacteriocin, limits both *Salmonella* and *Listeria***
354 **pathogenesis**

355 Treatment of the Caco-2 cells with the purified bacteriocin inhibited STM, STY, and LM
356 invasion and fold proliferation without compromising host-cell viability (Fig. 8, A-D).
357 Additionally, the purified bacteriocin treatment inhibited STM biofilm formation in a dose-
358 dependent manner alongside reduced transcript level expression of *Salmonella* biofilm
359 regulatory genes (Fig. S8, A-D). Moreover, bacteriocin treatment (10µg/ml) attenuated
360 *Salmonella* virulence gene expression such as SPI-1 gene- *sipC*, SPI-2 gene-*pipB2,* and
361 flagellar gene *fliC* (Fig. S8, E-G). Subsequently, TEM imaging revealed a complete loss of
362 *Listeria* flagella upon treatment with the OS-derived bacteriocin in contrast to *Salmonella*
363 which retained few flagella even on bacteriocin treatment (Fig. 8, E-H). Furthermore, the
364 motility assay demonstrated a significant swimming defect of *Listeria* and *Salmonella* upon
365 treatment with either OS supernatant or bacteriocin to the untreated control (Fig. 8, I-J).
366 Overall, our study depicts the novel role of OS-derived bacteriocin in limiting *Salmonella* and
367 *Listeria* invasion and pathogenesis by regulating virulence effectors such as SPI-1, SPI-2
368 genes, biofilm regulatory genes, and flagella.

369 **DISCUSSION**

370 *Salmonella* gains access to the systemic sites by traversing the gut intestinal barrier via utilizing
371 several routes. Its primary site of entry is the distal ileum wherein it induces the SPI-1 Type
372 Three Secretion System (T3SS) effector proteins to facilitate its uptake. After its initial entry
373 into the enterocytes and M-cells overlying the Peyer's patches, *Salmonella* colonizes the
374 draining MLN and eventually disseminates to the liver and spleen via the circulating

375 lymphatics and the bloodstream (40). *Salmonella* uptake by M cells facilitates its stealthy entry
376 via avoidance of the mucus barrier. Additionally, the presence of flagella allows them to propel
377 through the viscous mucus and activate the immune responses(16). The initial induction of pro-
378 inflammatory responses during activation of cell-death pathways promotes systemic
379 dissemination (40) (41, 42). The onset of systemic dissemination coincides with GVB
380 disruption and loss of tight-junction protein expression (1). Several reports have suggested the
381 protective role of gut commensals in maintaining gut epithelial health against food-borne
382 pathogen insults. *E. coli* provide colonization resistance against STM in the presence of a
383 specific microbial consortium by limiting galactitol wherein *Lachnospiraceae* consume the
384 free sugar, conferring colonization resistance (43). Similarly, the commensal *Klebsiella*
385 *michiganensis* retention or transmission provided colonization resistance to Enterobacteriaceae
386 by exhibiting nutrient competition (44). In this study, we report the broad-spectrum protective
387 role of the gut commensal of bacteroidales order *O. splanchnicus* against *Salmonella* and
388 *Listeria* colonization, pathogenesis, and dissemination by inhibiting GVB damage,
389 angiogenesis, inflammatory responses, and tight junction disruption in mice. Additionally, not
390 only OS but its culture supernatant could exert its inhibitory effect on *Salmonella* invasion and
391 intracellular proliferation in intestinal human epithelial cells. Moreover, the OS and its
392 supernatant could inhibit STM biofilm formation by regulating flagella formation. This STM
393 biofilm inhibitory effect was however lost upon co-culture with paraformaldehyde-fixed-OS
394 indicating the presumable role of certain inhibitory microbial products secreted by
395 metabolically live OS. Further, our studies identified OS-produced bacteriocins responsible for
396 restricting intracellular replication of *Salmonella* and *Listeria* in intestinal epithelial cells by
397 regulating bacterial virulence arsenals such as biofilm regulatory genes, SPI-1, SPI-2 genes,
398 and flagellar machinery. However, the presence of flagella on *Salmonella* post bacteriocin
399 treatment hints towards the possibility of other secreted accessory molecules within the OS

400 supernatant and warrants future research. Due to the proteinaceous nature of the bacteriocin,
401 oral administration experiments in mice were aborted. This study provides evidence about
402 inter-species regulation of gut colonization in maintaining gut homeostasis and protecting
403 against several invading pathogens. Moreover, the long-term protective ability conferred by
404 OS during pre-or post-infection colonization to mice against broad-spectrum foodborne
405 pathogens such as *Salmonella* and *Listeria* highlights its therapeutic potential as a prebiotic for
406 prophylaxis or post-infection treatment option, paving the way for future therapeutic
407 interventions to thwart food-borne infections.

408 **MATERIALS AND METHODS**

409 **Bacterial Strains and Culture Conditions**

410 *Salmonella* enterica serovar Typhimurium (STM) strain ATCC 14028S, STM ATCC 14028S
411 constitutively expressing mCherry (pFPV25.1-mCherry-Amp^R, RFP), laboratory stock of
412 *Enterococcus faecalis* (Ef), *Shigella flexneri*, *Listeria monocytogenes* expressing mCherry and
413 *Odoribacter splanchnicus* (OS) strain NCTC 10825 [1651/6] from ATCC were used in this
414 study. 4% paraformaldehyde-fixed-OS was used as killed bacteria control. The STM live
415 bacterial strain was grown overnight in LB broth at 37 ^{0}C under 160 rpm shaking condition.
416 OS was cultured in anaerobic condition in tryptic soy broth at 37ºC for 48h after its revival
417 from glycerol stock.

418 **Preparation of Cell-free Bacterial Culture Supernatant**

419 The overnight grown OS culture in tryptic soy broth was centrifuged at 10,000rpm for 10 min
420 and the supernatant was harvested. The collected supernatant was further subjected to another
421 two rounds to centrifugation to remove any residual cells. The supernatant was subsequently
422 filtered using a 0.2 µm filter and stored at − 20˚C.

423

424 **Animal Experiment**

425 The animal experiments were conducted in accordance with the approved guidelines of the
426 institutional animal ethics committee at the Indian Institute of Science, Bangalore, India
427 (Registration No: 48/GO/ReRcBiBt-S/Re-L/99/CPCSEA). All procedures involving the use of
428 animals were performed according to the Institutional Animal Ethics Committee (IAEC)-
429 approved protocol (CAF/Ethics/853/2021). 6–8 weeks old adult C57BL/6 male mice were used
430 in this study. After one day of OS colonization (10^5 CFU/mice orally), the mice were infected
431 with 10^6 (organ burden) CFU or 10^7 CFU (for assessing survival) of *S.* Typhimurium, 10^8
432 (organ burden) or 10^9 (survival) CFU of *L. monocytogenes* or 10^7 (organ burden) or 10^8
433 (survival) CFU of *S. flexneri* orally. The colonization of *O. splanchnicus* was confirmed via
434 RT-qPCR mediated quantitation of OS 16S rRNA from the mice fecal and ileal samples.
435 Infected mice were subjected to intraperitoneal injection of either 1 mg/kg body weight of
436 SIRT1 inhibitor EX-527 (Sigma-Aldrich), or SIRT3 inhibitor 3TYP (Selleck Chemical) or
437 vehicle control alone on every alternate day. For post-infection OS administration studies, OS
438 was orally administered (10^5 CFU/ mice) post 1 or 3dpi. 5-day post-infection, mice were
439 euthanized, dissected out, and blood and organs were harvested. The bacterial organ load was
440 enumerated by plating the tissue homogenates on *Salmonella-Shigella* (SS) agar plates for
441 *Salmonella* or *Shigella* or LB plates containing 50µg/ml of Ampicillin for LM. The harvested
442 tissues and the fecal samples were collected in protein lysis buffer and TRIzol (Takara) for
443 protein and RNA extraction respectively and were stored at -80ºC. For calculating percentage
444 survival, the infected mice cohorts were monitored till fatality and fatalities were reported.

445 **ELISA**

446 Estimation of cytokines in mice serum was performed according to the manufacturer's
447 instructions. Briefly, 96-well ELISA plates (BD Bioscience) were coated overnight with

capture antibody at 4°C. Following day, plates were washed with 0.1% Tween-20 containing PBS and blocked with 10% FBS for 1 h. Following blocking, wells were washed and incubated with 50µl of serum samples in duplicates for 2 h at room temperature. Subsequently, plates were washed and incubated with detection antibody and enzyme reagent for 1 h at room temperature (BD Bioscience). TMB (Sigma) was used as a substrate and reactions were stopped with 2 N H_2SO_4. For the estimation of IL-1β, pre-coated ELISA (SARD Biosciences) plates were used, and ELISA was performed as per manufacturer's protocol.

Absorbance was measured at 450 nm wavelength in Tecan Plate reader and the concentration of cytokines were interpolated from a standard curve.

Quantitative Real Time PCR

Total RNA was isolated from tissues harvested in TRIzol (Takara) as per manufacturer's protocol. RNA was quantified using Nano Drop (Thermo-Fischer scientific). Integrity of isolated RNA was detected by performing 2% agarose gel electrophoresis. 3 µg of total isolated RNA was subjected to DNaseI (Thermo Fischer Scientific) treatment at 37°C for 1 hr followed by heat inactivation at 75°C in the presence of 5mM concentration of EDTA for 10 mins. The mRNA was reverse transcribed to cDNA using oligo $(dT)_{18}$ primer, buffer, dNTPs and reverse transcriptase (Takara) as per manufacturer's protocol. The expression profile of target gene was evaluated using specific primers (Table-S2) by using SYBR green RT-PCR master mix (Takara) in Applied Biosystems (Quantstudio 5) or BioRad Real time PCR instrument. β-actin was used as an internal control for mammalian genes and for bacterial genes 16S rRNA was used. All the reaction was setup in 384 well plate with three replicates for each sample.

Western blotting

The harvested tissue samples were lysed in ice-cold RIPA buffer (50 mM Tris-Cl, pH 8.0, 150 mM NaCl, 5mM EDTA, 1% NP-40, 1 % Sodium deoyxycholate, 1% SDS) containing protease

473 inhibitor cocktail (Roche). Total protein was estimated using Bradford reagent (BioRad).
474 Protein samples were denatured in **Laemmli SDS loading buffer** at 95ºC for 10 min and then
475 subjected to separation on 12% SDS-PAGE gels followed by transfer onto activated 0.45µm
476 PVDF membrane. Finally, the membrane was blocked with 5% skimmed milk in TBST (Tris
477 Buffered Saline containing 0.1% Tween-20) and probed with appropriate primary (Table-S3)
478 and secondary HRP-conjugated antibodies. The blots were developed using ECL substrate
479 (Bio-Rad) using a Chemidoc (BioRad). All densitometric analysis was performed using
480 ImageJ software.

481 **Immunohistochemistry**

482 The harvested tissues were fixed in 4% paraformaldehyde, embedded in paraffin and 5 µm
483 thick paraffin sections were collected on poly-lysine coated glass slides. The sectioned tissue
484 samples were deparaffinized using standard protocol. Primary antibody staining of the
485 deparaffinized sections was performed with specific primary antibody in the presence of a
486 permeabilizing agent, 0.01% saponin (Sigma) dissolved in 2.5% BSA containing PBS at 4°C
487 for overnight. Following wash with PBS, sections were stained with appropriate secondary
488 antibody tagged with fluorochrome for 1 hr at RT. This was followed by DAPI staining and
489 mounting. For in vivo estimation of biofilm, deparaffinized tissue samples were stained with
490 Calcofluor White (Sigma) stain for 20 min at RT. All immunofluorescence images were
491 obtained using Zeiss multi-photon 880 microscope and were analyzed using ZEN black 2012
492 software.

493 **Haematoxylin and Eosin Staining**

494 The harvested tissues were collected and fixed using 3.5% paraformaldehyde. The fixed liver
495 was then dehydrated using a gradually increasing concentration of ethanol and embedded in

496 paraffin. 5µm sections were collected on coated plates. Sections were further rehydrated and
497 then stained with hematoxylin and eosin. Images were collected in a Leica microscope.

498 **Cell Culture**

499 Human colorectal adenocarcinoma cell line Caco-2 were maintained in Dulbecco's Modified
500 Eagle's Media (DMEM) (Lonza) and supplemented with 10% FCS (Fetal calf serum, Gibco)
501 and 1% non-essential amino acid solution (Sigma Aldrich) at 37ºC temperature in the presence
502 of 5% CO_2 in humidified incubator. Prior to each experiment, cells were seeded into 24 well
503 or 6 well plate as per requirement at a confluency of 60%.

504 **Intracellular proliferation or gentamicin protection assay**

505 Caco-2 epithelial were infected with 3 to 4 h old log phase *S.* Typhimurium (STM) bacterial
506 culture, STM with *O. splanchnicus*, STM in presence of *O. splanchnicus* supernatant and STM
507 along with PFA-fixed OS at an MOI of 10. For attachment of bacteria to the cells, tissue culture
508 plates were subjected to centrifugation at 600xg for 5 min and incubated at 37 ^{0}C humified
509 incubator with 5% CO_2 for 25 min. Following infection of the cells with STM at an MOI of 10,
510 cells were treated with DMEM (Sigma) + 10% FBS (Gibco) containing 100 µg/ml gentamicin
511 for 1 hr. Subsequently, the gentamicin concentration was reduced to 25 µg/ml and maintained
512 until the specified time point. Post 2hr and 16hr post-infection, cells were lysed in 0.1% triton-
513 X-100. Lysed cells were serially diluted and plated on *Salmonella-Shigella* (SS) agar to obtain
514 colony-forming units (cfu). Percent invasion was determined using the following formula:

515 **Percent invasion= [CFU at 2 h]/ [CFU of pre-inoculum] X 100**

516 Fold proliferation was calculated as cfu at 16hr divided by cfu at 2hr.

517 **Fold Proliferation= [CFU at 16h] / [CFU at 2h]**

518 **Immunofluorescence confocal microscopic studies**

At the specified time points post infection with mCherry-tagged STM, or GFP-tagged OS or with both mCherry-STM and GFP-OS, cells were fixed with 3.5% paraformaldehyde for 15 min. Primary antibody staining was performed with specific primary antibody in the presence of a permeabilizing agent, 0.01% saponin (Sigma) dissolved in 2.5% BSA containing PBS at 4°C for overnight or for 6hr at room temperature (RT). Following this, cells were washed with PBS stained with appropriate secondary antibody tagged with fluorochrome for 1 hr at RT. This was followed by DAPI staining and mounting of the coverslip onto a clean glass slide using the mounting media containing the anti-fade agent. The coverslip sides were sealed with a transparent nail paint. All immunofluorescence images were obtained using Zeiss Multiphoton 880 and were analyzed using ZEN black 2012 software.

Growth Curve analysis

For *in vitro* growth curve experiments a single colony of STM and OS was inoculated in 5mL of LB broth singly or in co-culture and grown overnight at 37ºC in anaerobic jar. In another set, STM was inoculated in 5mL of LB in presence of OS supernatant. Overnight-grown stationary phase bacteria were sub-cultured at a ratio of 1: 100 in freshly prepared LB in presence or absence of OS supernatant and kept at 37ºC. At different time intervals, aliquots were taken for measurement of [OD]600nm by TECAN 96 well microplate reader and were plated for CFU enumeration.

Growth conditions for biofilm formation

LB medium devoid of NaCl (i.e. 1% casein enzyme hydrolysate (Hi-Media, India) and 0.5% yeast extract (Hi-Media, India), devoid of NaCl) was used as biofilm media. Overnight grown culture were subcultured in 2 ml biofilm medium at the dilution of 1:100 in a flat-bottom 24-well polystyrene plate (Tarsons, India) and incubated at 28˚C for 72 h without shaking.

Bacterial Biofilm inoculation with culture supernatant

To test the effect OS culture supernatant on biofilm formation, 20 µl of STM WT overnight culture and indicated volume (1% v/v and/or as indicated in the figures) of the OS culture supernatants was added to 2 ml of biofilm media,and incubated under biofilm inducing condition. For co-culture experiments, the overnight cultures of the STM and OS or STM and PFA-fixed OS were added in a 1:1 ratio to 2 ml of biofilm media and incubated under biofilm-inducing conditions.

Crystal Violet Staining

Post 72 h of biofilm induction, the media was discarded, and the plates were thoroughly washed in water. The plates were dried, and 2 ml of 1% Crystal Violet (CV) was added to each well and incubated for 15 min. Post 15 min incubation, the CV stain was removed, and the plate was thoroughly rinsed in water to remove excess stain. The stained biofilm was destained with 70% ethanol, and the intensity of the colour of the destained solution was quantified at OD_{595} in the Tecan plate reader (Infinite Pro 200).

Glass bead assay

1 mm glass beads were added onto the pellicle to assess the strength of the pellicle at the air-liquid interface. The initial weight of the glass beads was noted. The glass beads were added until the pellicle collapsed, and the final weight was noted down and plotted.

Gut Permeability Assay

The infected mice cohorts were orally administered with FITC Dextran (25mg/kg,FD-4-100MG, Sigma) 4h before euthanization. The blood plasma was collected post-euthanization by cardiac puncture followed by centrifugation. The blood plasma was evaluated for mean fluorescence via plate reader (TECAN) and flow cytometry(CytoFlex, Beckman).

MTT Assay

Post-16h treatment of pre-seeded Caco-2 cells with 10µg/ml of bacteriocin, MTT staining solution (0.5mg/ml) was added to each well followed by incubation at 37ºC CO_2incubator for 4h. 50µl of DMSO was added per well for solubilizing the formazan crystals. Absorbance was measured at 570nm using a plate reader (TECAN).

Transmission electron microscopy

Overnight STM or LM-grown cultures (in the presence or absence of OS supernatant or bacteriocin) were subcultured into fresh media (1:10) ratio and incubated at 37ºC for 6 hours under shaking conditions. These samples were centrifugated at 1000rpm for 10 min to obtain the bacterial pellet. The bacterial pellet was subjected to PBS wash twice via centrifugation at 1000 rpm for 10 min.5 µl of the finally resuspended cell suspension was added on a glow-discharged copper-grid, air dried, stained with 1% uranyl acetate for 30 s, and visualized under a transmission electron microscope (JEM-100 CX II; JEOL).

Supernatant Treatment

The supernatant was treated with 7.5 mM concentrations of EDTA and incubated at 65 ℃ for 1 h. To 200 µl of supernatant, 10 µl of proteinase-K (NEB, stock 20 mg/ml) was added and incubated at 37 ℃ for 1 h. The proteinase was inactivated with 0.5 mM PMSF and incubated at 28 ℃ for 1 h. The supernatant was heated to 37˚C (60 min), 65˚C (15 min) or 95˚C (15 min) for the indicated time and immediately frozen at − 20˚C. Post-treatment, the supernatants were used to inoculate the biofilm to test the nature of the biofilm inhibitory molecules.

Supernatant concentration and separation based on molecular weight

4 ml of the supernatants were transferred to the Amicon ultra filter device (Amicon® Ultra-4 centrifugal filter device, 3k MWCO, UFC800324; Amicon® Ultra-4 Centrifugal filter Unit, 10k MWCO, UFC801024) and centrifuged at 4000 g for 30 min in a swing bucket rotor. The concentrated solute from the bottom of the filter device and the flowthrough were collected by a pipette and subjected to biofilm inoculation.

Size Exclusion Chromatography

The bacterial supernatant was concentrated to 0.5ml using 3k MWCO-Amicon-Ultra-4-centrifugal unit and loaded onto the Superdex 200pg size exclusion column (XK16/60, 124mL; Cytiva, USA), pre-equilibrated Tris-Cl buffer (pH-8) containing 100mM NaCl and 20mM Tris-Cl. The sample was eluted with the same buffer at a flow rate of 0.8mL/min, and 1mL fractions were collected. The fractions corresponding to the elution peaks were analyzed for biofilm inhibition activity and subjected to mass spectrometry.

LC/MS analysis of the supernatant fractions

The concentrated gel filtration fractions of supernatants were subjected to in-solution trypsin digestion for LC Q-TOF MS analysis. Briefly, 100 µg of total protein was resuspended in 100 µl of 7-8M of urea buffer. To this, 5 µl 200mM DTT was added and incubated at room temperature for 1 hr, followed by alkylation with 20µl of 200 mM iodoacetamide and incubation at room temperature for 1h in the dark. This was followed by the addition of 1mM of Calcium chloride and incubation at RT for 10 min. For protein digestion, trypsin solution was added to the sample to a final trypsin to protein ratio of 1:30 (w/w) and incubated at 37˚C for 16 h, with frequent shaking. The reaction was stopped by adding 0.1% formic acid to adjust the pH to 3-4. The digested protein samples were desalted using a reverse phase C-18 column

(Acclaim prep EASY-Spray (C18-RP)) using mobile phase solvent A-2% acetonitrile and solvent B- 80% acetonitrile. The sample injection volume was 10µl. All the samples were analyzed using Thermo Scientific SII for Xcalibur method. The MS scan was acquired using Orbitrap detector with 60000 resolution in the positive polarity and scan range (*m/z*) 350-2000. The ion source type was NSI with static voltage; positive ion (V)- 2200V and negative ion (V)- 600 along with temperature settings at 275ºC. This was followed by $ddMS^2$ IT HCD with 30% fragmentation HCD collision energy using ion trap detector. The raw data was analyzed using Proteome Discoverer 2.5 against the *O. splanchnicus* proteome available in UniProt (Proteome ID: UP000006657).

Purification of bacteriocin

O. splanchnicus culture supernatant was concentrated within the range of >3kDa and <10kDa using the Amicon Ultra-4 Centrifugal filter units of 10MWCO and 3MWCO. The concentrated cell-free supernatant containing the bacteriocin (~7kDa) was precipitated by ammonium sulphate (80% to 98%). The precipitate was collected by centrifugation at 12000rpm for 30 min and dissolved in 1X PBS. The dissolved precipitate was again filtrated using the 3KDa cutoff Amicon centrifugal filter units. This concentrated fraction was further subjected to Fast Performance Liquid Chromatography using Superdex 75 Increase 10/300 GL- 24ml volume (GE Healthcare) column. The column was equilibrated with 1X Phosphate Buffered Saline buffer and 0.5ml of concentrated sample (23.6 mg/ml) was injected into the column. Based on the increase in Absorbance units at 280nm from baseline, 0.3ml fractions were collected at a retention volume of 13.3ml to 21.8ml (Fig. S9). The fractions were analyzed by 20% SDS-PAGE electrophoresis and stained with Coomassie staining solution.

***In vitro* swim motility assay**

2 µl of treated or untreated bacterial samples were spotted on the 0.3% agar (LB-STM, BHI-LM) plates supplemented with 0.5% yeast extract, 1% casein enzyme hydrolysate, 0.5% NaCl, and 0.5% glucose. The plates were incubated at 37˚C and images were taken every 6 h (STM) or 24h (LM) using the camera of Biorad illuminator.

Statistical analysis

Data were analyzed and graphed using the GraphPad Prism 8 software (San Diego, CA). Statistical significance was determined by Student's t-test or Two way ANOVA and Bonferroni post-t-test to obtain p values. Adjusted p-values below 0.05 are considered statistically significant. The results are expressed as mean ± SD or SEM of three independent experiments.

REFERENCES

1. Spadoni I, Zagato E, Bertocchi A, Paolinelli R, Hot E, Di Sabatino A, et al. A gut-vascular barrier controls the systemic dissemination of bacteria. Science. 2015;350(6262):830-4.
2. Brescia P, Rescigno M. The gut vascular barrier: a new player in the gut–liver–brain axis. Trends in Molecular Medicine. 2021;27(9):844-55.
3. Ghosh S, Whitley CS, Haribabu B, Jala VR. Regulation of Intestinal Barrier Function by Microbial Metabolites. Cellular and Molecular Gastroenterology and Hepatology. 2021;11(5):1463-82.
4. Zhao Y, Chen F, Wu W, Sun M, Bilotta AJ, Yao S, et al. GPR43 mediates microbiota metabolite SCFA regulation of antimicrobial peptide expression in intestinal epithelial cells via activation of mTOR and STAT3. Mucosal immunology. 2018;11(3):752-62.
5. Schulthess J, Pandey S, Capitani M, Rue-Albrecht KC, Arnold I, Franchini F, et al. The short chain fatty acid butyrate imprints an antimicrobial program in macrophages. Immunity. 2019;50(2):432-45. e7.
6. Hajra D, Rajmani RS, Chaudhary AD, Gupta SK, Chakravortty D. Salmonella-induced SIRT1 and SIRT3 are crucial for maintaining the metabolic switch in bacteria and host for successful pathogenesis. eLife Sciences Publications, Ltd; 2024.
7. Garcia-del Portillo F, Foster JW, Finlay BB. Role of acid tolerance response genes in Salmonella typhimurium virulence. Infection and immunity. 1993;61(10):4489-92.
8. Haraga A, Ohlson MB, Miller SI. Salmonellae interplay with host cells. Nat Rev Microbiol. 2008;6(1):53-66.
9. Hensel M. Evolution of pathogenicity islands of Salmonella enterica. International journal of medical microbiology : IJMM. 2004;294(2-3):95-102.
10. Hiippala K, Barreto G, Burrello C, Diaz-Basabe A, Suutarinen M, Kainulainen V, et al. Novel Odoribacter splanchnicus Strain and Its Outer Membrane Vesicles Exert Immunoregulatory Effects in vitro. Frontiers in microbiology. 2020;11:575455.
11. Xing C, Wang M, Ajibade AA, Tan P, Fu C, Chen L, et al. Microbiota regulate innate immune signaling and protective immunity against cancer. Cell host & microbe. 2021;29(6):959-74.e7.

12. Balakrishnan A, Schnare M, Chakravortty D. Of men not mice: bactericidal/permeability-increasing protein expressed in human macrophages acts as a phagocytic receptor and modulates entry and replication of Gram-negative bacteria. Frontiers in immunology. 2016;7:455.
13. Chatterjee R, Chowdhury AR, Nair AV, Hajra D, Kar A, Datey A, et al. Salmonella Typhimurium PgtE is an essential arsenal to defend against the host resident antimicrobial peptides. Microbiological research. 2023;271:127351.
14. Davis CW, Dickey BF. Regulated airway goblet cell mucin secretion. Annual review of physiology. 2008;70:487-512.
15. Enss ML, Cornberg M, Wagner S, Gebert A, Henrichs M, Eisenblätter R, et al. Proinflammatory cytokines trigger MUC gene expression and mucin release in the intestinal cancer cell line LS180. Inflammation research : official journal of the European Histamine Research Society [et al]. 2000;49(4):162-9.
16. McGuckin MA, Lindén SK, Sutton P, Florin TH. Mucin dynamics and enteric pathogens. Nature reviews Microbiology. 2011;9(4):265-78.
17. Hill RR, Cowley HM, Andremont A. Influence of colonizing micro-flora on the mucin histochemistry of the neonatal mouse colon. The Histochemical journal. 1990;22(2):102-5.
18. Cash HL, Whitham CV, Behrendt CL, Hooper LV. Symbiotic bacteria direct expression of an intestinal bactericidal lectin. Science (New York, NY). 2006;313(5790):1126-30.
19. Goubier A, Dubois B, Gheit H, Joubert G, Villard-Truc F, Asselin-Paturel C, et al. Plasmacytoid Dendritic Cells Mediate Oral Tolerance. Immunity. 2008;29(3):464-75.
20. Müller-Redetzky HC, Suttorp N, Witzenrath M. Dynamics of pulmonary endothelial barrier function in acute inflammation: mechanisms and therapeutic perspectives. Cell and tissue research. 2014;355(3):657-73.
21. Daneman R, Rescigno M. The gut immune barrier and the blood-brain barrier: are they so different? Immunity. 2009;31(5):722-35.
22. Wang Y, Rattner A, Zhou Y, Williams J, Smallwood PM, Nathans J. Norrin/Frizzled4 signaling in retinal vascular development and blood brain barrier plasticity. Cell. 2012;151(6):1332-44.
23. Liebner S, Corada M, Bangsow T, Babbage J, Taddei A, Czupalla CJ, et al. Wnt/beta-catenin signaling controls development of the blood-brain barrier. The Journal of cell biology. 2008;183(3):409-17.
24. Simmons DL, Satterthwaite AB, Tenen DG, Seed B. Molecular cloning of a cDNA encoding CD34, a sialomucin of human hematopoietic stem cells. Journal of immunology (Baltimore, Md : 1950). 1992;148(1):267-71.
25. Pusztaszeri MP, Seelentag W, Bosman FT. Immunohistochemical expression of endothelial markers CD31, CD34, von Willebrand factor, and Fli-1 in normal human tissues. The journal of histochemistry and cytochemistry : official journal of the Histochemistry Society. 2006;54(4):385-95.
26. Oehlers SH, Cronan MR, Scott NR, Thomas MI, Okuda KS, Walton EM, et al. Interception of host angiogenic signalling limits mycobacterial growth. Nature. 2015;517(7536):612-5.
27. Iwase T, Uehara Y, Shinji H, Tajima A, Seo H, Takada K, et al. Staphylococcus epidermidis Esp inhibits Staphylococcus aureus biofilm formation and nasal colonization. Nature. 2010;465(7296):346-9.
28. Lee J, Jayaraman A, Wood TK. Indole is an inter-species biofilm signal mediated by SdiA. BMC microbiology. 2007;7(1):1-15.
29. Fux CA, Costerton JW, Stewart PS, Stoodley P. Survival strategies of infectious biofilms. Trends in microbiology. 2005;13(1):34-40.
30. Costerton JW, Stewart PS, Greenberg EP. Bacterial biofilms: a common cause of persistent infections. Science (New York, NY). 1999;284(5418):1318-22.
31. Hajra D, Nair AV, Chakravortty D. An elegant nano-injection machinery for sabotaging the host: Role of Type III secretion system in virulence of different human and animal pathogenic bacteria. Physics of life reviews. 2021;38:25-54.

32. Chandra K, Nair AV, Chatterjee R, Muralidhara P, Singh A, Kamanna S, et al. Absence of proline-peptide transporter YjiY in Salmonella Typhimurium leads to secretion of factors which inhibits intra-species biofilm formation. Microbiological research. 2023;273:127411.
33. Jennings ME, Quick LN, Ubol N, Shrom S, Dollahon N, Wilson JW. Characterization of Salmonella type III secretion hyper-activity which results in biofilm-like cell aggregation. PloS one. 2012;7(3):e33080.
34. Ducarmon QR, Zwittink RD, Hornung BVH, van Schaik W, Young VB, Kuijper EJ. Gut Microbiota and Colonization Resistance against Bacterial Enteric Infection. Microbiology and molecular biology reviews : MMBR. 2019;83(3).
35. Caballero-Flores G, Pickard JM, Núñez G. Microbiota-mediated colonization resistance: mechanisms and regulation. Nature Reviews Microbiology. 2023;21(6):347-60.
36. Qin J, Li R, Raes J, Arumugam M, Burgdorf KS, Manichanh C, et al. A human gut microbial gene catalogue established by metagenomic sequencing. Nature. 2010;464(7285):59-65.
37. Gewolb IH, Schwalbe RS, Taciak VL, Harrison TS, Panigrahi P. Stool microflora in extremely low birthweight infants. Archives of disease in childhood Fetal and neonatal edition. 1999;80(3):F167-73.
38. Heilbronner S, Krismer B, Brötz-Oesterhelt H, Peschel A. The microbiome-shaping roles of bacteriocins. Nature reviews Microbiology. 2021;19(11):726-39.
39. Cotter PD, Ross RP, Hill C. Bacteriocins - a viable alternative to antibiotics? Nature reviews Microbiology. 2013;11(2):95-105.
40. Watson KG, Holden DW. Dynamics of growth and dissemination of Salmonella in vivo. Cellular microbiology. 2010;12(10):1389-97.
41. Monack DM, Hersh D, Ghori N, Bouley D, Zychlinsky A, Falkow S. Salmonella exploits caspase-1 to colonize Peyer's patches in a murine typhoid model. The Journal of experimental medicine. 2000;192(2):249-58.
42. Fink SL, Cookson BT. Pyroptosis and host cell death responses during Salmonella infection. Cellular microbiology. 2007;9(11):2562-70.
43. Eberl C, Weiss AS, Jochum LM, Durai Raj AC, Ring D, Hussain S, et al. E. coli enhance colonization resistance against Salmonella Typhimurium by competing for galactitol, a context-dependent limiting carbon source. Cell host & microbe. 2021;29(11):1680-92.e7.
44. Oliveira RA, Ng KM, Correia MB, Cabral V, Shi H, Sonnenburg JL, et al. Klebsiella michiganensis transmission enhances resistance to Enterobacteriaceae gut invasion by nutrition competition. Nat Microbiol. 2020;5(4):630-41.

763

764

765 **MAIN FIGURES**

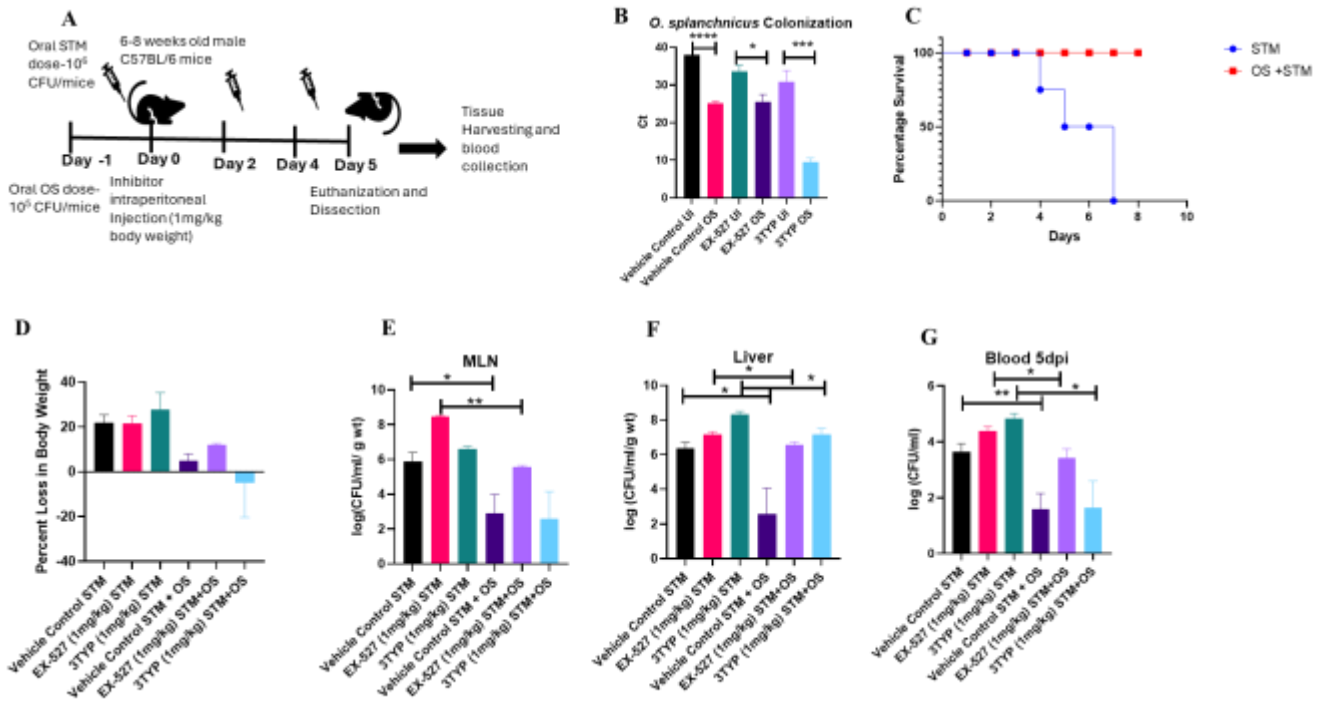

766

767

768 **Figure 1. *Odoribacter splanchnicus* colonization protects mice from *Salmonella***

769 **colonization and dissemination**

770 A-Schematic representation showing animal experimental strategy of infection.

771 B-OS colonization validation via qPCR quantification of *O. splanchnicus* 16S rRNA from fecal

772 samples of mice.

773 C-Survival percentage of non-colonized-STM-infected mice versus OS-colonized-STM-

774 infected mice cohorts. Data is represantative of N=2, n=5.

775 D-Percent weight loss exhibited by OS colonized and non-colonized mice upon STM infection

776 at 5th day post infection. Data is representative of N=3,n=5.

777 E-G- STM organ loads in MLN (E), liver (F) and blood (G) at 5th post-infection in OS colonized

778 and non-colonized mice cohorts in untreated, and SIRT1 (EX-527) or SIRT3 (3TYP) inhibitor

779 treatment. Data is representative of N=3, n=3. Mann Whitney Test was performed to obtain p-

780 values.

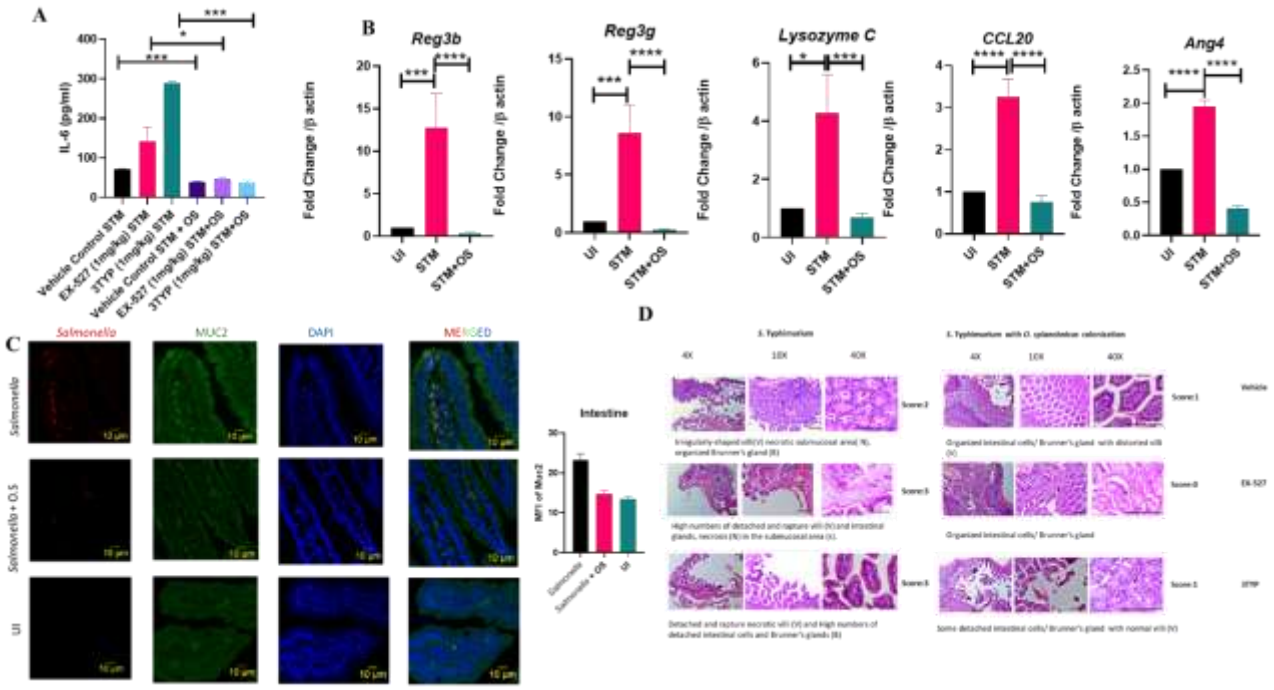

781

782 **Figure 2. *O. splanchnicus* reduces *Salmonella* induced inflammation and intestinal**

783 **damage**

784 A-Estimation of serum IL-6 production via ELISA upon STM infection in OS non-colonized

785 and colonized mice cohorts in presence or absence of SIRT1 or SIRT3 inhibitor treatment.

786 Unpaired t-test is performed to obtain the p-values. Data is representative of N=2, n=5.

787 B-Quantitative gene expression data of several antimicrobial peptides (AMPs) precursor genes

788 in uninfected and STM-infected mice intestinal tissues harvested at 5th dpi from OS colonized

789 or non-colonized cohorts. Unpaired t-test is performed to obtain the p-values. Data is
790 representative of N=2, n=5.

791 C- Immunostaining representing Muc2 protein expression in intestinal tissues of OS non-
792 colonized and colonized mice cohorts upon STM infection.

793 D-Haematoxylin-eosin-stained intestinal sections harvested from STM-infected OS non-
794 colonized or colonized mice cohorts at 5th dpi. 0-represents normal pathology, 1- represents-
795 mild pathology, 2-3-represents severe pathology.

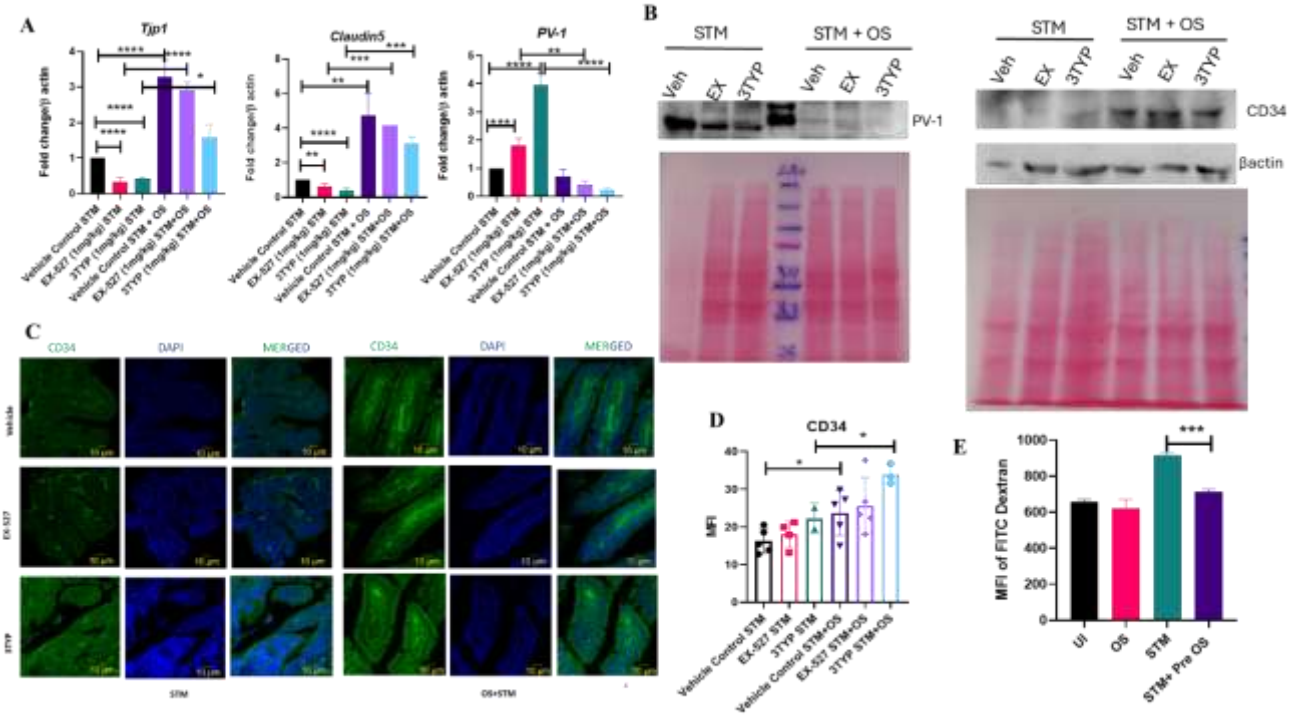

796

797 **Fig 3. *Odoribacter splanchnicus* gut colonization prevents *Salmonella*-induced GVB**
798 **damage by promoting tight junction gene expression.**

799 A-Quantitative gene expression studies of tight junction protein complexes (*Tjp1*, *Claudin5*)
800 and PV-1 gene (marker of GVB damage) in STM-infected mice intestinal tissue in presence or
801 absence of OS gut colonization.

802 B-Immunoblotting depicting expression of PV-1 and CD34 protein in intestinal tissues of OS
803 non-colonized and colonized mice cohorts upon STM infection.

804 C-Immunohistochemistry representing CD34 (endothelial marker of vasculature) protein
805 expression in intestinal tissues of OS non-colonized and colonized mice cohorts upon STM
806 infection.

807 D-Quantitative representation of the Median Fluorescence Intensity (MFI) of CD34 protein
808 expression in intestinal immunohistochemical sections shown in (C). Data is representative of
809 N=2,n>50. Un-paired t-test was used to obtain the p-values.

810 E- Estimation of FITC fluorescence in mice plasma via gut permeability assay in infected mice
811 cohorts upon oral administration of FITC Dextran (25mg/kg) 4h before euthanization at 5th day
812 post *Salmonella* infection.

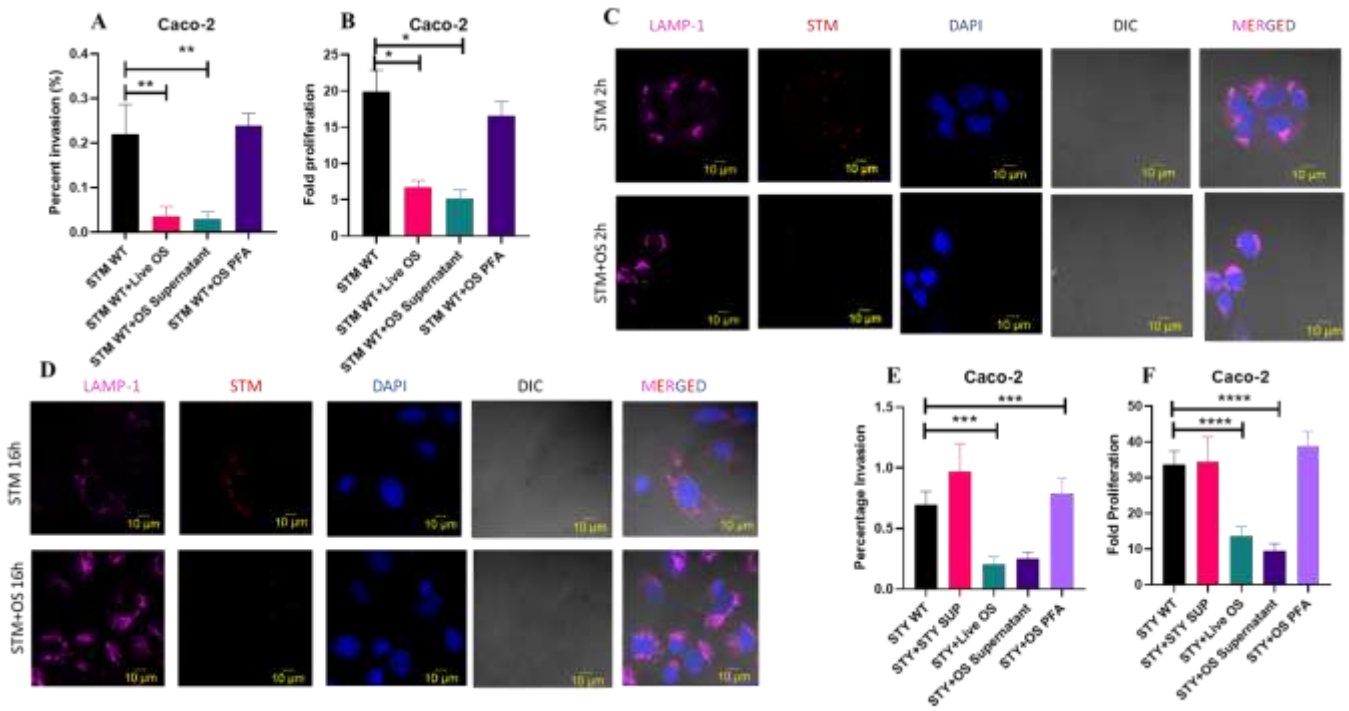

813

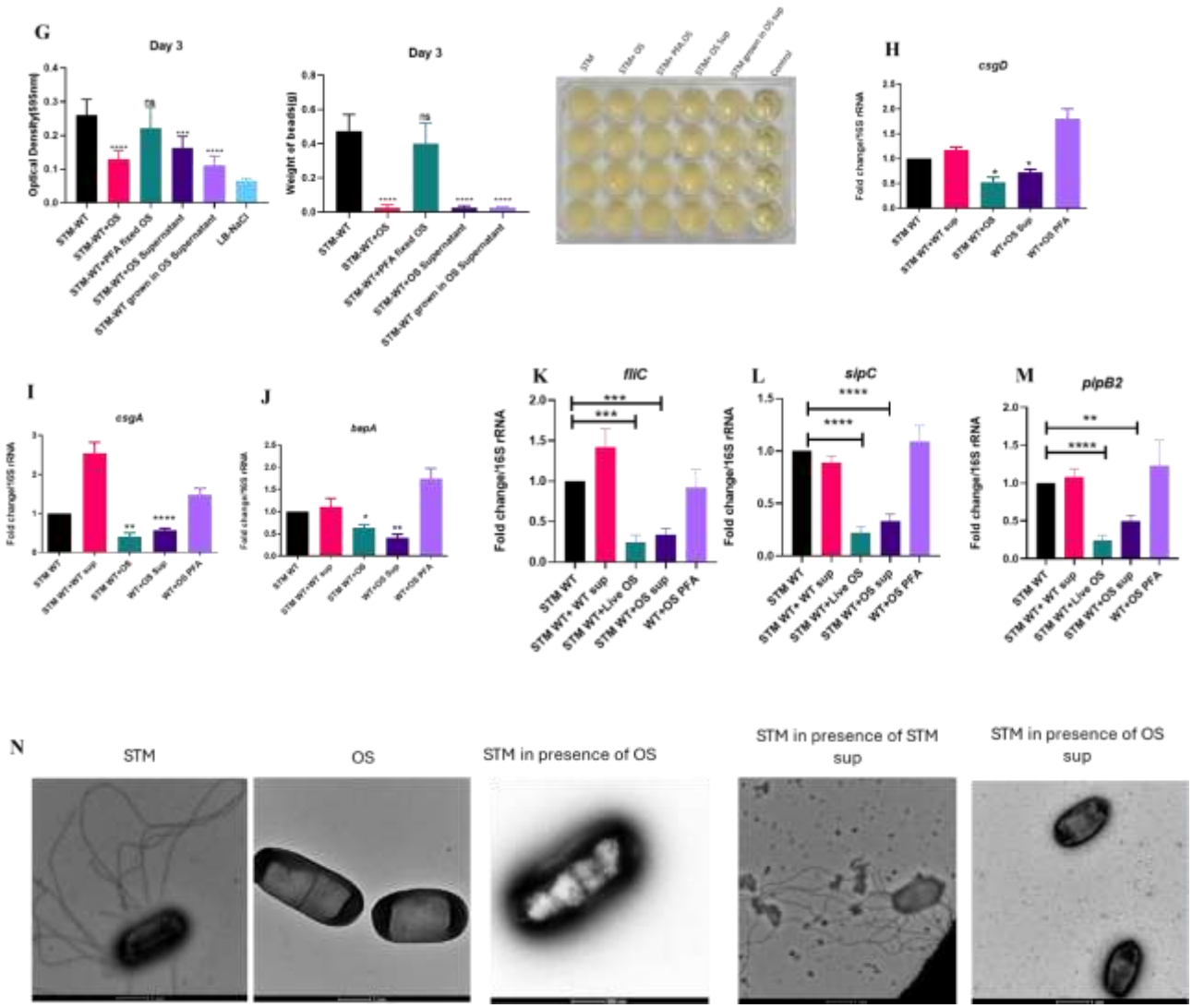

Fig 4. *O. splanchnicus* exhibits its inhibitory effect on *Salmonella* biofilm formation and inhibits invasion and intracellular replication in human intestinal cells

A-Percent invasion of STM in human Caco-2 human intestinal cells in presence or absence of live OS, OS culture supernatant, PFA-fixed-OS. Data is representative of N=3, n=3. Unpaired t-test is used to obtain the p-values.

B-Intracellular proliferation of STM Caco-2 cells in presence or absence of live OS, OS culture supernatant, PFA-fixed-OS. Data is representative of N=3, n=3. Unpaired t-test is used to obtain the p-values.

824 C- Representative immunofluorescence images depicting STM invasion into Caco-2 cells in
825 presence or absence of OS at 2hr post-infection. Data is representative of N=3, n=100.
826 Unpaired t-test is used to obtain the p-values.

827 D- Representative immunofluorescence images depicting STM invasion into Caco-2 cells in
828 presence or absence of OS at 2hr post-infection. Data is representative of N=3, n=100.
829 Unpaired t-test is used to obtain the p-values.

830 E-Percent invasion of STY in Caco-2 human cells in presence or absence of OS, OS culture
831 supernatant, PFA-fixed OS. Data is representative of N=3, n=3. Unpaired t-test is used to obtain
832 the p-values.

833 F-Intracellular proliferation of STY in Caco-2 cells in presence or absence of live OS, OS
834 culture supernatant, PFA-fixed-OS. Data is representative of N=3, n=3. Unpaired t-test is used
835 to obtain the p-values.

836 G- Biofilm assay showing the biofilm formation ability of STM-WT or STM-WT grown in OS
837 supernatant after 72h of inoculation in presence or absence of live OS, OS culture supernatant,
838 PFA-fixed-OS. Data is representative of N=4, n=4. Unpaired t-test is used to obtain the p-
839 values. Image of the STM biofilm formed plate in the above stated conditions has been shown.

840 H-M- RT-qPCR mediated gene expression of STM biofilm regulatory genes (*csgD*) (H), *csgA*
841 (I), *bapA* (J), along with flagellar gene (*fliC*) (K), SPI-1 (*sipC*) (L) and SPI-2 (*pipB2*) (M)
842 genes in presence or absence of live OS or its spent media or PFA-fixed-OS. Data is
843 representative of N=2, n=5. Unpaired Student's t-test was used to obtain the p-values.

844 N- Transmission Electron Microscopic (TEM) images of STM in presence or absence of
845 *Salmonella* WT supernatant, OS and its supernatant to assess the possession of flagella.

846

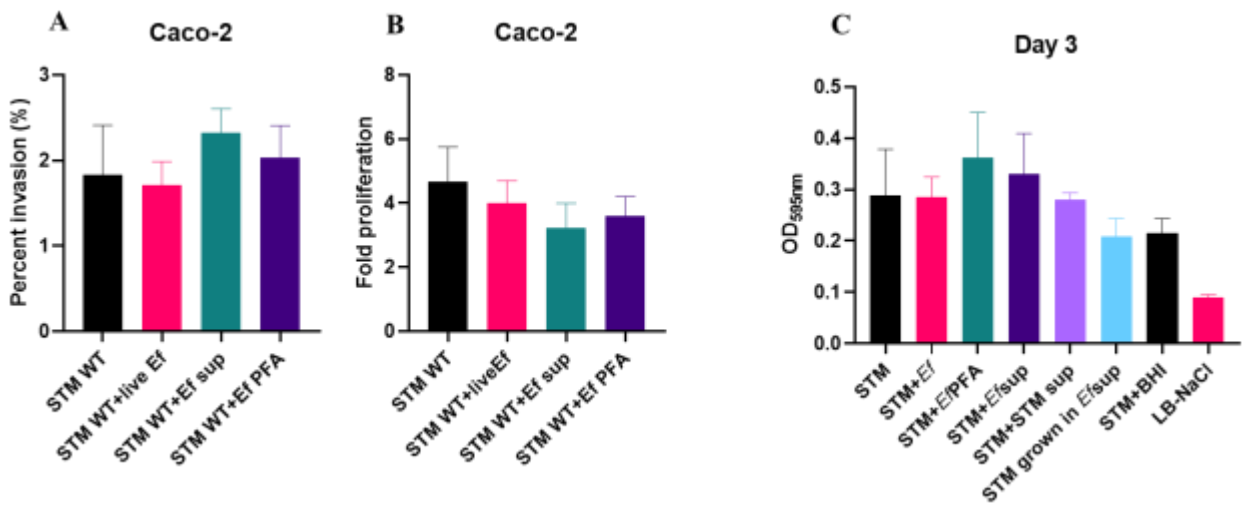

Fig 5. Unlike *O. splanchnicus, E. faecalis* fail to exert any inhibitory effect on *Salmonella in vitro* biofilm formation or *Salmonella* invasion and intracellular replication in human intestinal cells

A-Percent invasion of STM in Caco-2 cells in presence or absence of live *E. faecalis* (Ef), Ef culture supernatant, PFA-fixed-Ef. Data is representative of N=3, n=3. Unpaired t-test is used to obtain the p-values.

B-Intracellular proliferation of STM in Caco-2 cells in presence or absence of live Ef, Ef culture supernatant, PFA-fixed-Ef. Data is representative of N=3, n=3. Unpaired t-test is used to obtain the p-values.

C. Biofilm assay depicting the biofilm formation ability of STM-WT or STM-WT grown in Ef supernatant after 72h of inoculation in presence or absence of live Ef, Ef or STM culture supernatant, PFA-fixed. Crystal-violet staining was performed to assess the biofilm formation on the solid-liquid interphase and the $[OD]_{595}$ absorbance reading was recorded. Data is representative of N=4, n=4. Unpaired t-test is used to obtain the p-values.

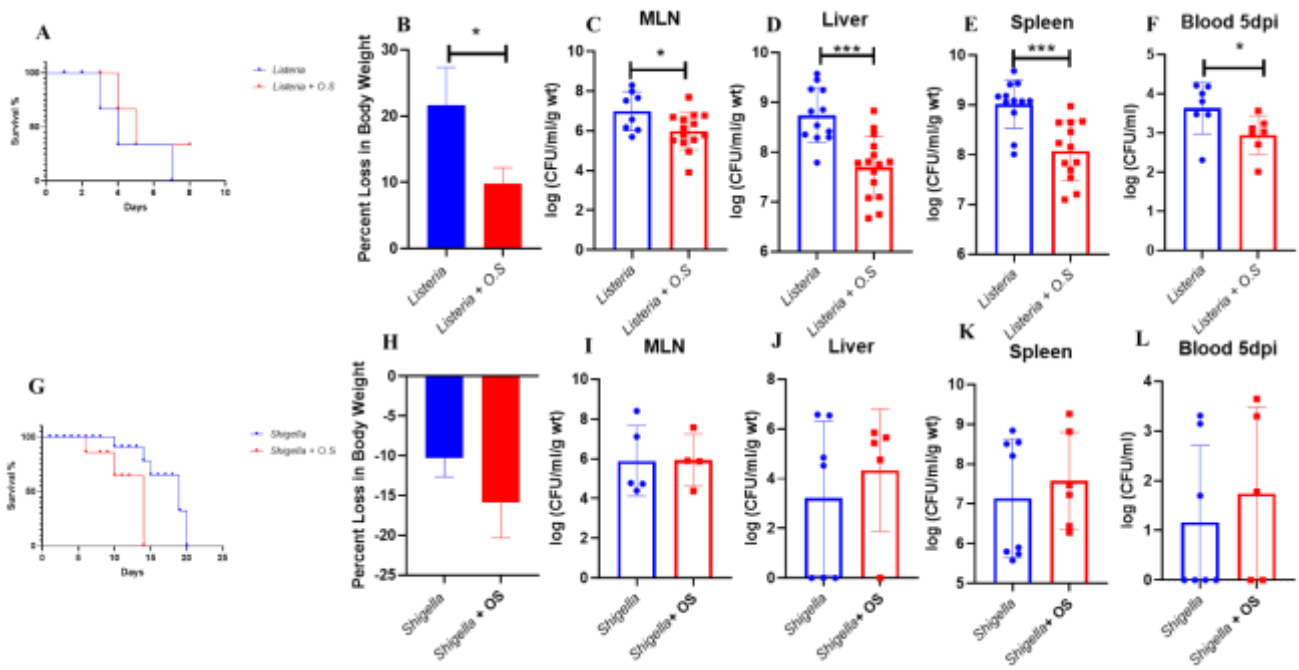

Fig 6. *Odoribacter splanchnicus* exerts its protective role against *Listeria monocytogenes* but not against *Shigella flexneri* in mice

A- Survival percentage of non-colonized LM-infected mice versus OS-colonized *Listeria*-infected mice cohorts. Data is represantative of N=2, n=8.

B-Percent weight loss exhibited by OS colonized and non-colonized mice upon LM infection at 5th dpi. Data is representative of N=2,n=8.

C-F- LM organ loads in Mesenteric lymph Node (MLN) (C), liver (D), spleen (E) and blood (F) at 5th dp. in OS colonized and non-colonized mice cohorts Data is representative of N=2, n=8. Mann Whitney Test was performed to obtain p-values.

G- Survival percentage of non-colonized *Shigella*-infected mice versus OS-SF-infected mice cohorts. Data is represantative of N=2, n=8.

H-Percent weight loss exhibited by OS colonized and non-colonized mice upon *S. flexneri* infection at 5th dpi. Data is representative of N=2,n=8.

878 I-L- *S. flexneri* organ loads in Mesenteric lymph Node (MLN) (I), liver (J), spleen (K) and

879 blood (L) at 5th dpi in OS colonized and non-colonized mice cohorts. Data is representative of

880 N=2, n=8. Mann Whitney Test was performed to obtain p-values.

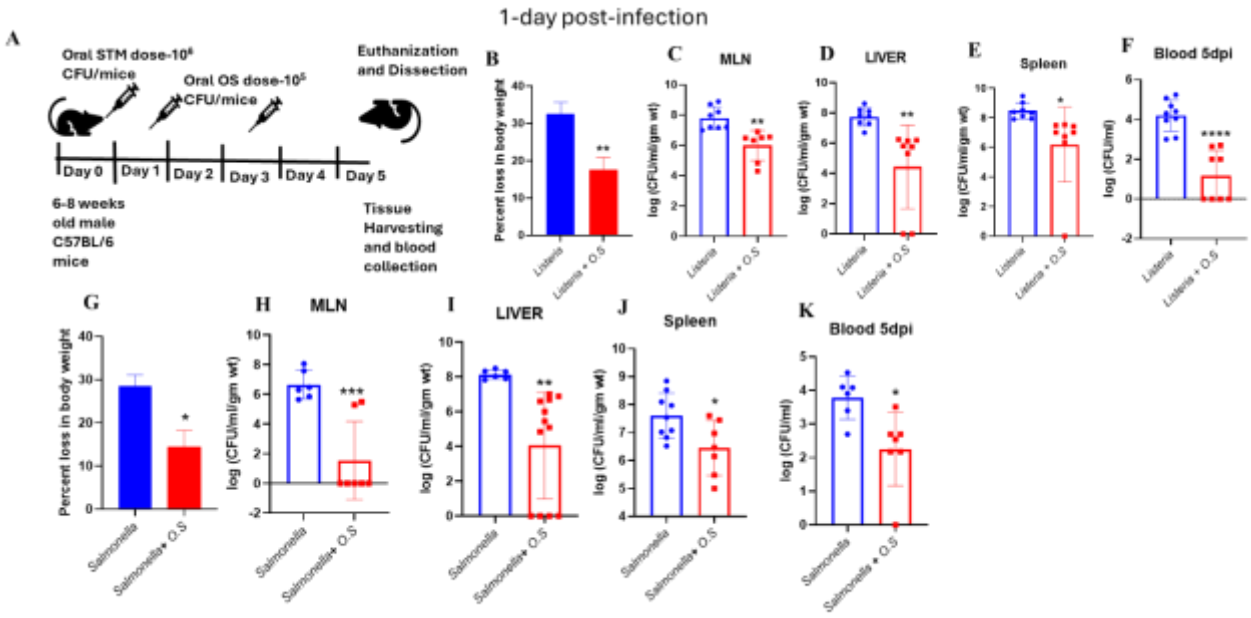

881

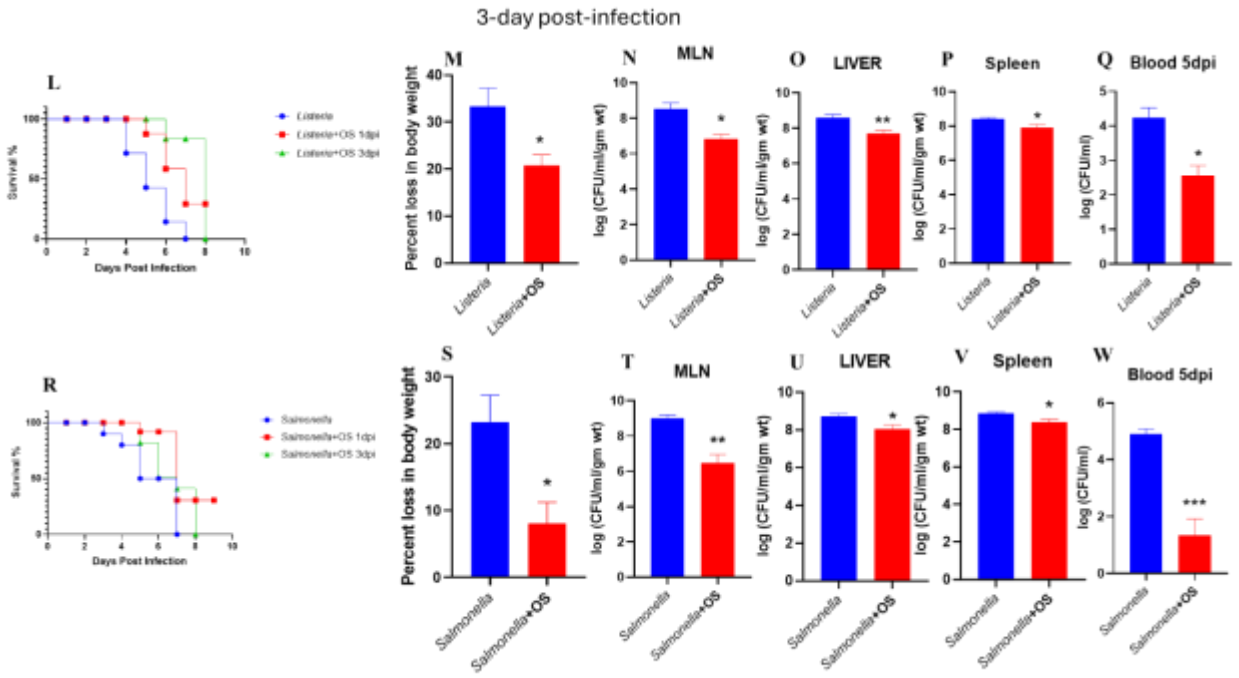

882

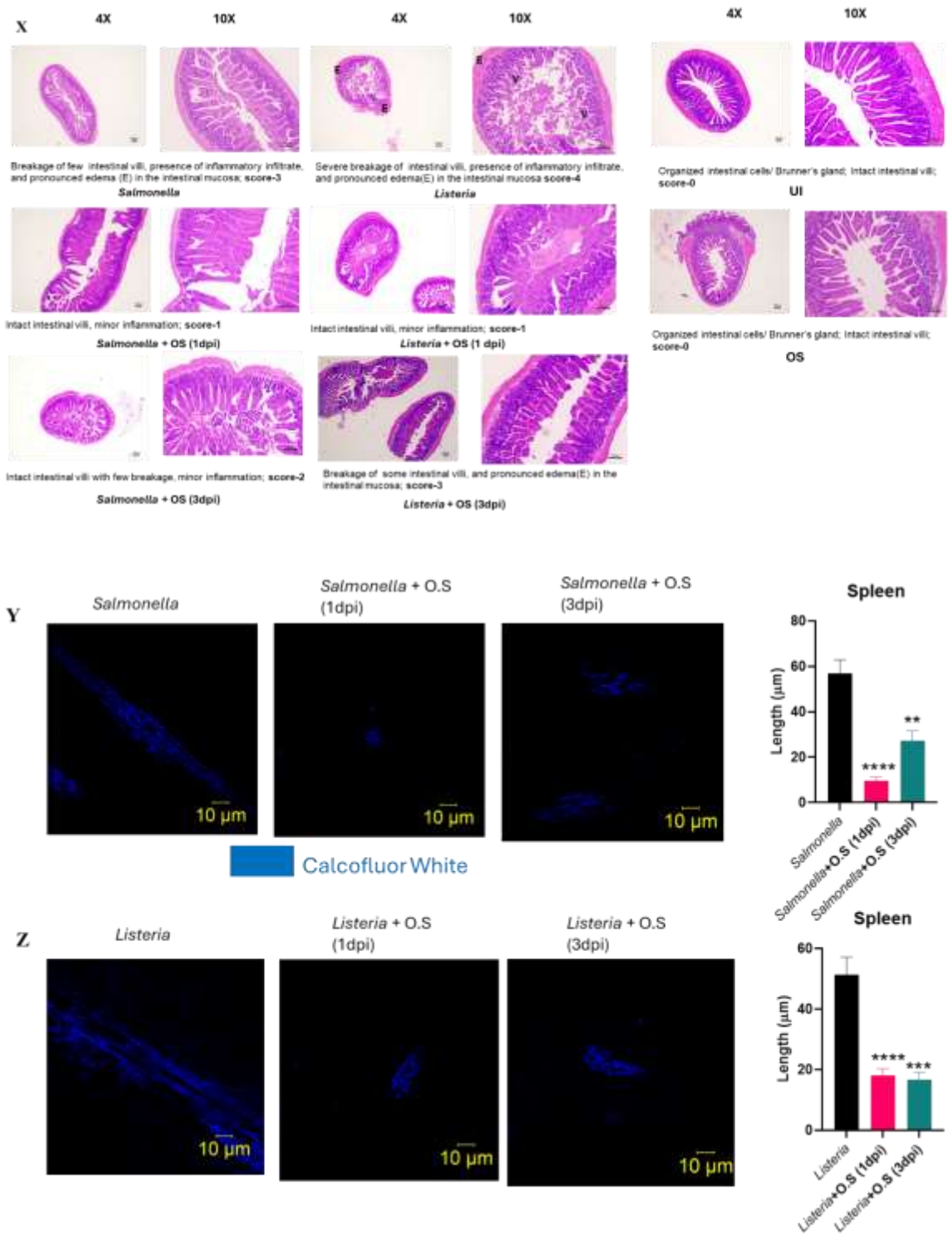

Fig. 7 *O. splanchnicus* even confers protection against foodborne pathogens when administered post-pathogenic challenge

A- Schematic representation showing the animal experimental strategy of infection.

888 B- Percent weight loss exhibited by OS colonized (1-dpi) and non-colonized mice upon LM
889 infection at 5th dpi. Data is representative of N=2,n=8.

890 C-F- LM organ loads in MLN (C), liver (D), spleen (E) and blood (F) at 5th dpi upon OS
891 administration at 1-dpi. Data is representative of N=2, n=8. Mann Whitney Test was performed
892 to obtain p-values.

893 G- Percent weight loss exhibited by OS colonized (1-dpi) and non-colonized mice upon STM
894 infection at 5th dpi. Data is representative of N=2,n=8.

895 H-K- STMorgan loads in MLN (H), liver (I), spleen (J) and blood (K) at 5th-dpi upon OS
896 administration at 1-dpi. Data is representative of N=2, n=8. Mann-Whitney Test was performed
897 to obtain p-values.

898 L- Survival percentage of non-colonized LM-infected mice versus OS-colonized (1 dpi or 3
899 dpi) *Listeria*-infected mice cohorts. Data is represantative of N=2, n=8.

900 M- Percent weight loss exhibited by OS colonized (3-dpi) and non-colonized mice upon LM
901 infection at 5th-day post-infection. Data is representative of N=2,n=8.

902 N-Q- LM organ loads in MLN (N), liver (O), spleen (P) and blood (Q) at 5th-dpi upon OS
903 administration at 3-dpi. Data is representative of N=2, n=8. Mann-Whitney Test was performed
904 to obtain p-values.

905 R- Survival percentage of non-colonized *Salmonella*-infected mice versus OS-colonized (1 dpi
906 or 3 dpi) *Listeria*-infected mice cohorts. Data is represantative of N=2, n=8.

907 **S**- Percent weight loss exhibited by OS-colonized (3-dpi) and non-colonized mice upon STM
908 infection at 5th-day post-infection. Data is representative of N=2,n=8.

909 T-W-STM organ loads in MLN (T), liver (U), spleen (V), and blood (W) at 5th-dpi upon OS
910 administration at 3-dpi. Data is representative of N=2, n=8. Mann-Whitney Test was performed
911 to obtain p-values.

912 **X-** Haematoxylin-eosin-stained intestinal sections harvested at 5th-dpi from Uninfected (UI) or
913 *Salmonella* or *Listeria*-infected mice cohorts having non-administered or administered OS (at
914 1st or 3rd dpi). 0-represents normal pathology, 1- represents- mild pathology, 2-3-represents
915 severe pathology.

916 **Y**- Representative Calcofluor white (CW) staining of STM-infected mice spleen tissues at 5th-
917 day post-infection with or without OS administration at 1st or 3rd dpi

918 **Z**- Representative CW staining of LM-infected mice spleen tissues at 5th-dpi with or without
919 OS administration at 1st or 3rd dpi.

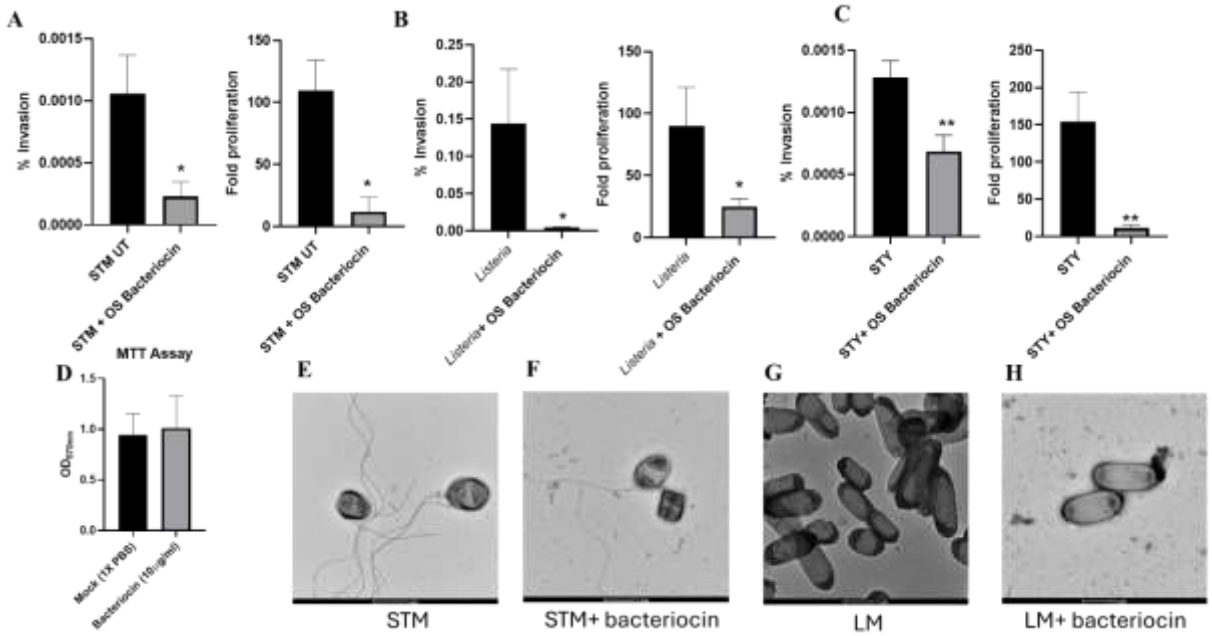

920

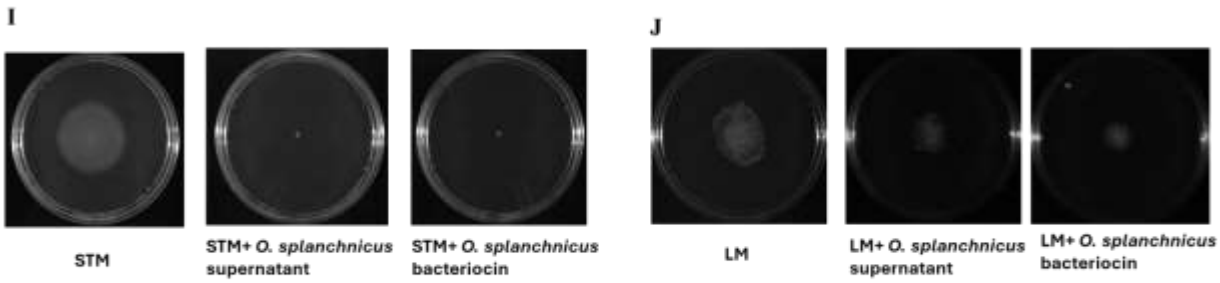

Fig. 8 *O. splanchnicus* bacteriocin restricts both *Salmonella* and *Listeria* pathogenesis

A- Percent invasion and intracellular fold proliferation of STM in Caco-2 cells under OS bacteriocin (10µg/ml) treatment. Data is representative of N=2, n=3. Unpaired t-test is used to obtain the p-values.

B- Percent invasion and intracellular fold proliferation of LM in Caco-2 cells under OS bacteriocin (10µg/ml) treatment. Data is representative of N=2, n=3. Unpaired t-test is used to obtain the p-values.

C- Percent invasion and intracellular fold proliferation of STY in Caco-2 cells under OS bacteriocin (10µg/ml) treatment. Data is representative of N=2, n=3. Unpaired t-test is used to obtain the p-values.

D-MTT assay evaluating the viability of Caco-2 cells upon 16h of mock or bacteriocin (10µg/ml) treatment. Data is representative of N=2, n=4.

E-F-TEM images of STM under untreated (D) or bacteriocin (10µg/ml) (E) treatment to assess the possession of flagella.

G-H- TEM images of LM under untreated (D) or bacteriocin (10µg/ml) (E) treatment to assess the possession of flagella.

I- Swimming motility assay of STM under OS supernatant or bacteriocin treatment.

J- Swimming motility assay of LM under OS supernatant or bacteriocin treatment.

List of Supplementary Materials

Fig. S1 to S9

Table S1 to S3

Acknowledgements:

We thank Nikhita Kirthivasan for her support during the commencement of the project.

We also thank our Divisional Mass Spectrometry facility, TEM facility, Departmental Confocal Facility, Divisional Flowcytometry Facility and Central Animal Facility at IISc.

Funding:

This work was supported by the DAE SRC fellowship (DAE00195) and DBT-IISc partnership umbrella program for advanced research in biological sciences and Bioengineering to DC.

Infrastructure support from ICMR (Centre for Advanced Study in Molecular Medicine), DST (FIST), UGC (special assistance) and TATA fellowship is highly acknowledged.

DH sincerely acknowledges the CSIR- SPM fellowship for her financial support.

The funders had no role in study design, data collection and analysis, decision to publish, or preparation of the manuscript.

Author contributions:

Conceptualization: DH, DC

Methodology: DH, DM, RV, VD (Gel Filtration Chromatography), DD (Fast Performance Liquid Chromatography)

Investigation: DH, DM, RV, VD (Gel Filtration Chromatography), DD (Size exclusion chromatography for bacteriocin purification), RSR (Scoring of haemoxylin and eosin-stained samples)

Visualization: DH, DM, RV

Funding acquisition: DC

Project administration: DH, DC

Supervision: DC, UT (Proteomics), TH (Size Exclusion Chromatography), MG (Size Exclusion Chromatography)

Writing – original draft: DH

Writing – review & editing: DH, DM, RV, RSR, VD, DD, TH, MG, UT, DC

Competing interests: Authors declare that they have no competing interests.

Data and materials availability:

All data are available in the main text or the supplementary materials.

SUPPLEMENTARY FIGURES

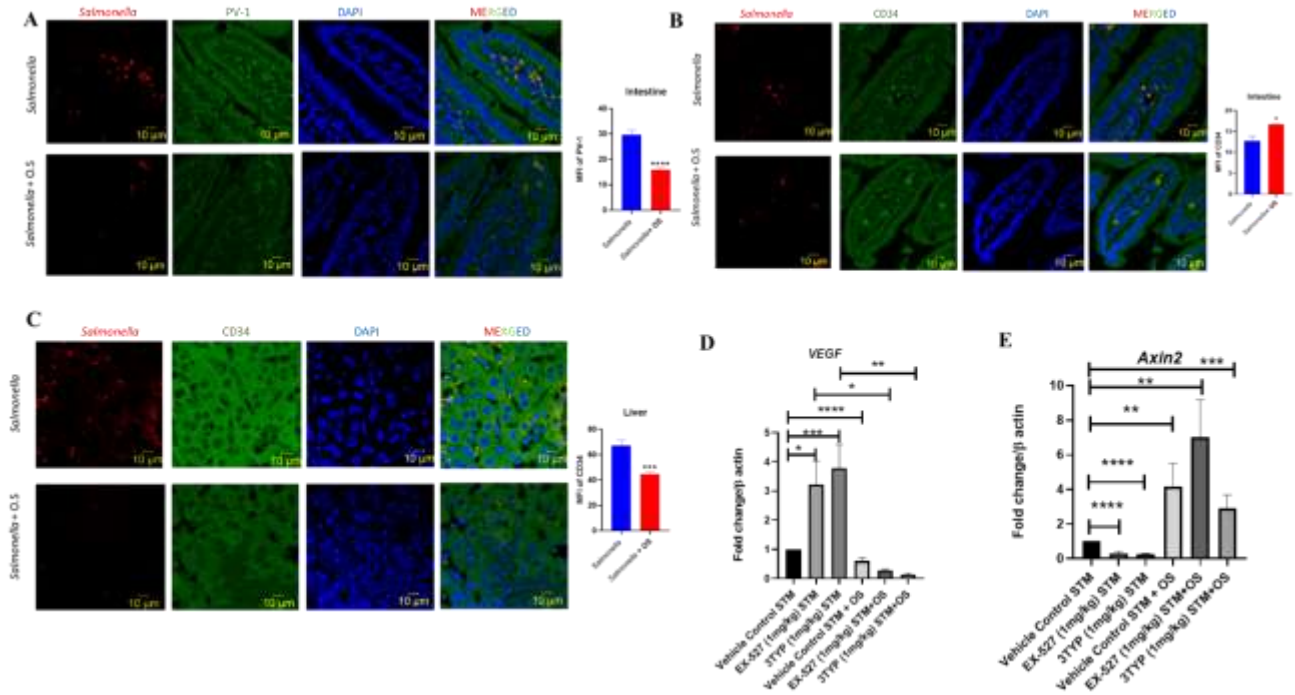

Fig S1. *O. splanchnicus* gut colonization prevents *Salmonella* dissemination by restricting intestinal GVB damage and angiogenesis

A-Immunohistochemistry demonstrating PV-1 protein expression in intestinal tissues of OS non-colonized and colonized mice cohorts upon STM infection.

B-C Immunohistochemical sections representing CD34 (an endothelial marker of vasculature) protein expression in intestinal (B) and liver (C) tissues of OS non-colonized and colonized mice cohorts upon STM infection. Data is representative of N=2, n=6 (tissue samples). Un-paired t-test was used to obtain the p-values.

D- qPCR mediated gene expression of pro-angiogenic marker *Vegf* in STM-infected mice liver tissues in presence or absence of OS pre-colonization. Data is representative of N=2, n=5. Un-paired t-test was used to obtain the p-values.

E- qPCR mediated gene expression of *Axin2* in STM-infected mice intestinal tissues in the presence or absence of OS pre-colonization. Data is representative of N=2, n=5. Un-paired t-test was used to obtain the p-values.

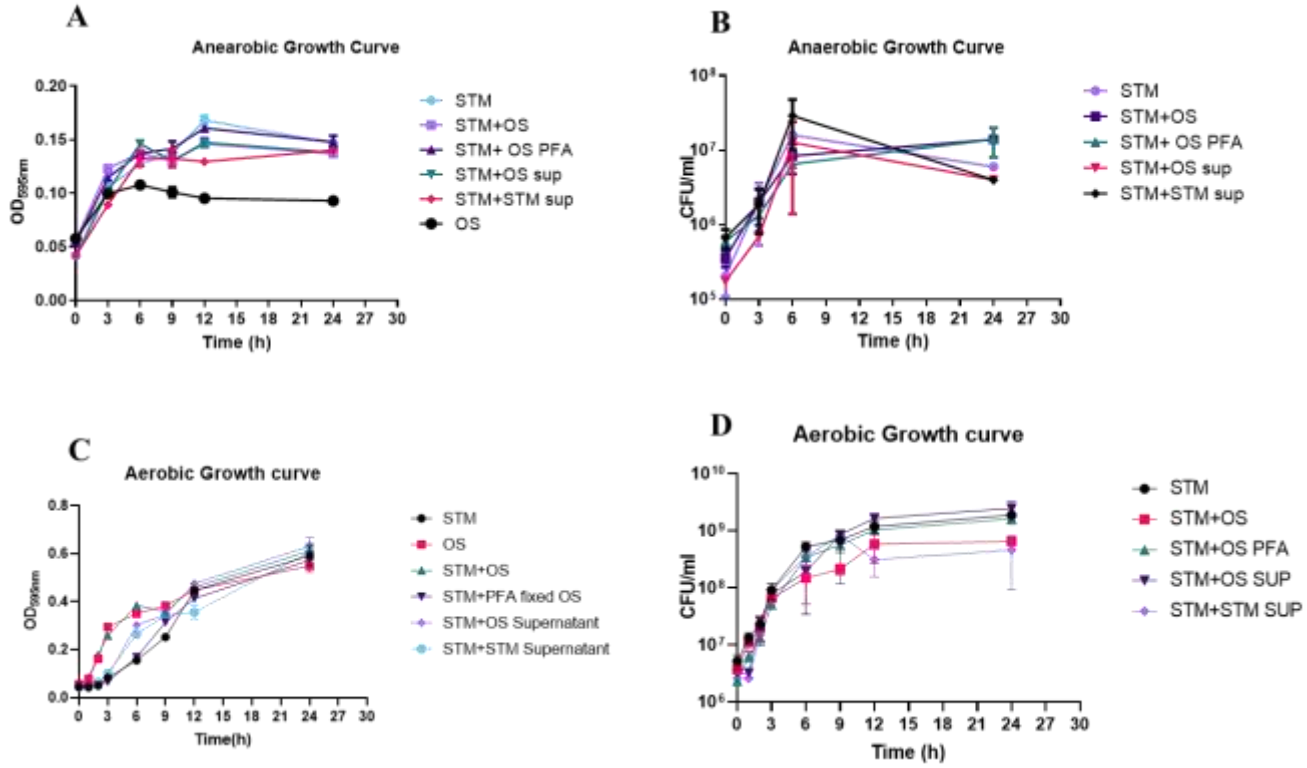

Fig. S2 In vitro growth kinetics of *Salmonella* Typhimurium in presence of live or dead *O. splanchnicus* or its culture supernatant

A-B Growth kinetics of STM-WT, OS, STM-WT in presence of OS, STM-WT in presence of STM or OS culture supernatant and STM-WT in presence of PFA-fixed OS in LB under anaerobic growth conditions.

C-D- Growth kinetics of STM-WT, OS, STM-WT in presence of OS, STM-WT in presence of STM or OS culture supernatant, STM-WT supernatant, and STM-WT in presence of PFA-fixed OS in LB under aerobic growth conditions.

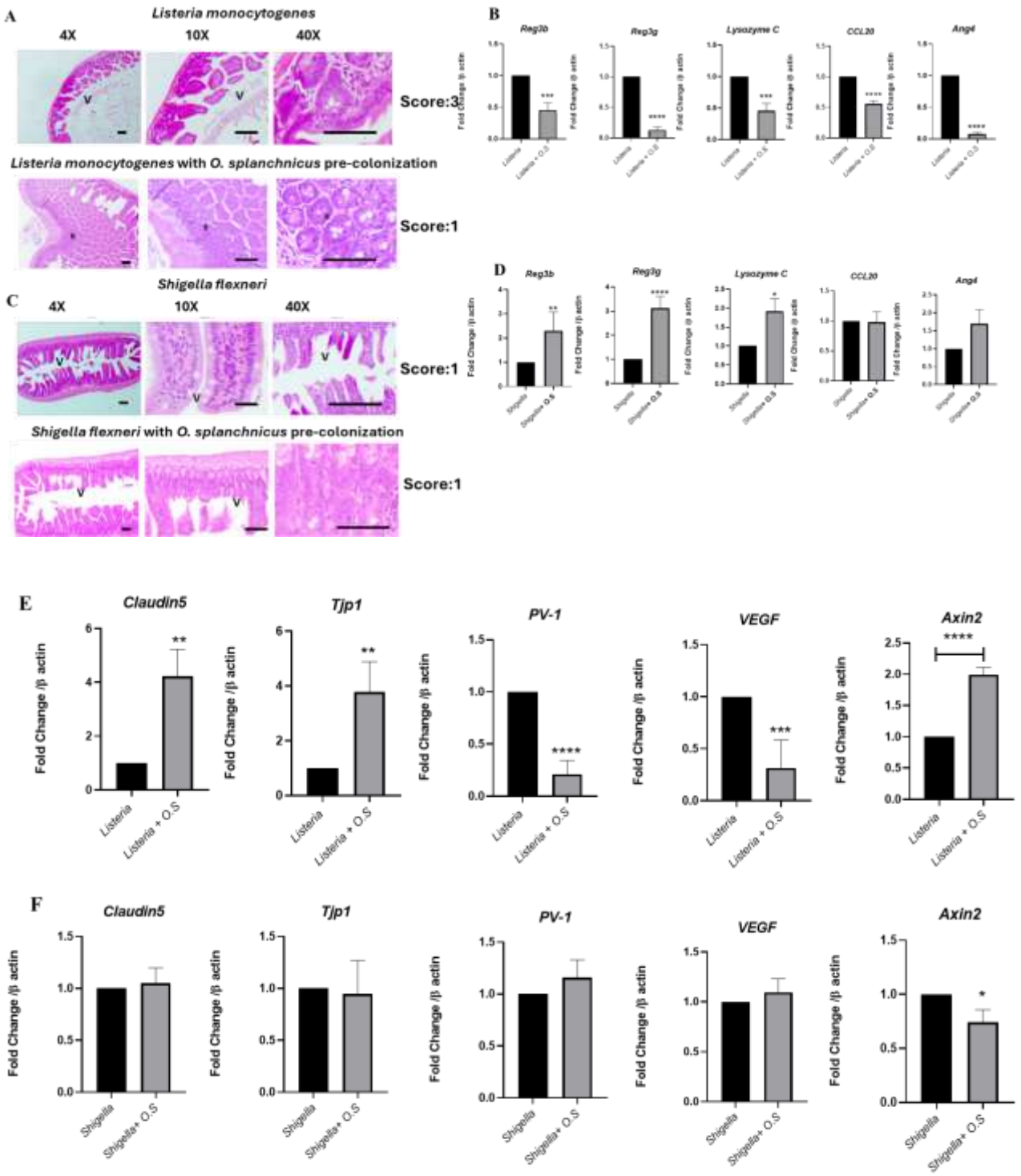
A
Listeria monocytogenes
4X
10X
40X
Score:3
Listeria monocytogenes with O. splanchnicus pre-colonization
Score:1
C
Shigella flexneri
4X
10X
40X
Score:1
Shigella flexneri with O. splanchnicus pre-colonization
Score:1
B
Reg3b
Reg3g
Lysozyme C
CCL20
Angl
D
Reg3b
Reg3g
Lysozyme C
CCL20
Angl
E
Claudin5
Tjp1
PV-1
VEGF
Axin2
Fold Change /β actin
Listeria
Listeria + O.S
F
Claudin5
Tjp1
PV-1
VEGF
Axin2
Fold Change /β actin
Shigella
Shigella+ O.S

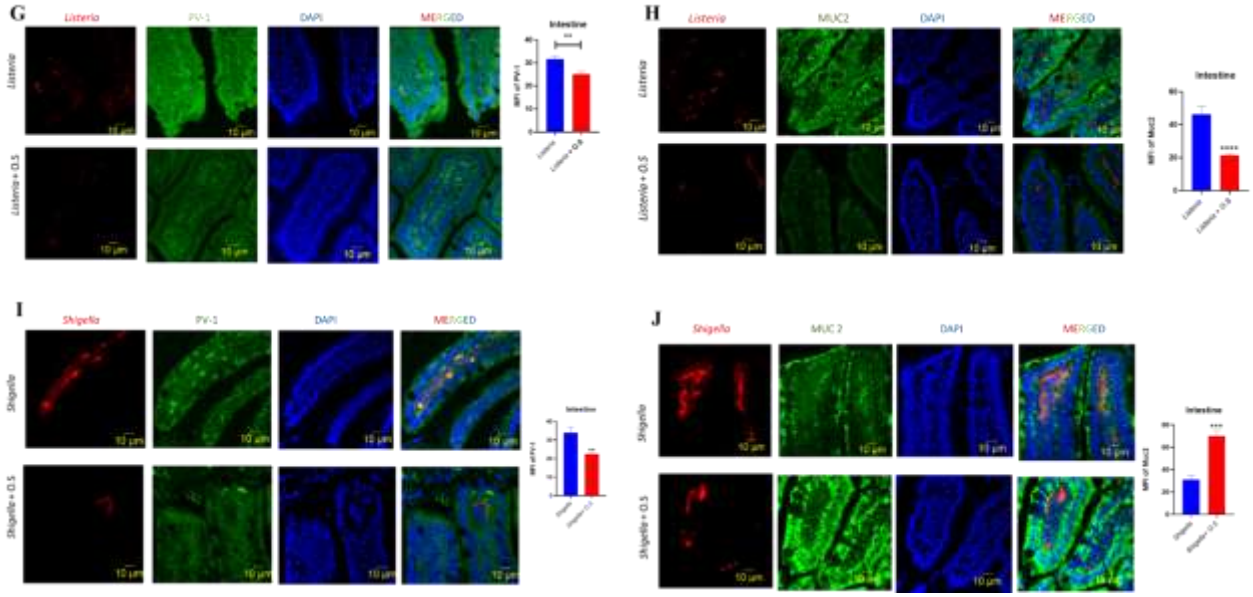
G
Listeria
PV-1
DAPI
MERGED
Listeria
Listeria + O.S
Intestine
H
Listeria
MUC2
DAPI
MERGED
Listeria
Listeria + O.S
Intestine
I
Shigella
PV-1
DAPI
MERGED
Shigella
Shigella + O.S
Intestine
J
Shigella
MUC 2
DAPI
MERGED
Shigella
Shigella + O.S
Intestine

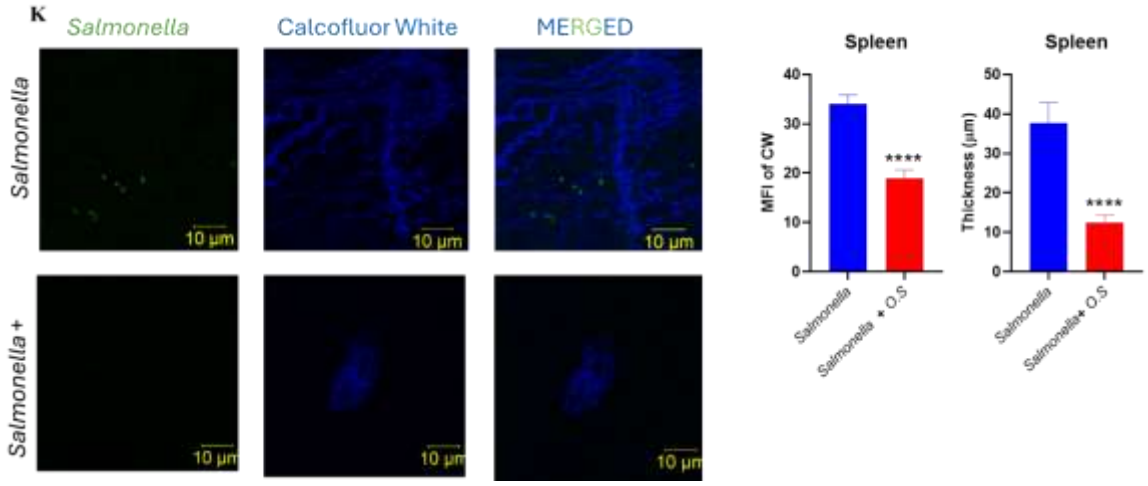
K
Salmonella
Calcofluor White
MERGED
Salmonella
Salmonella +
10 µm
Spleen
MFI of CW
Thickness (µm)
****
Salmonella
Salmonella + O.S

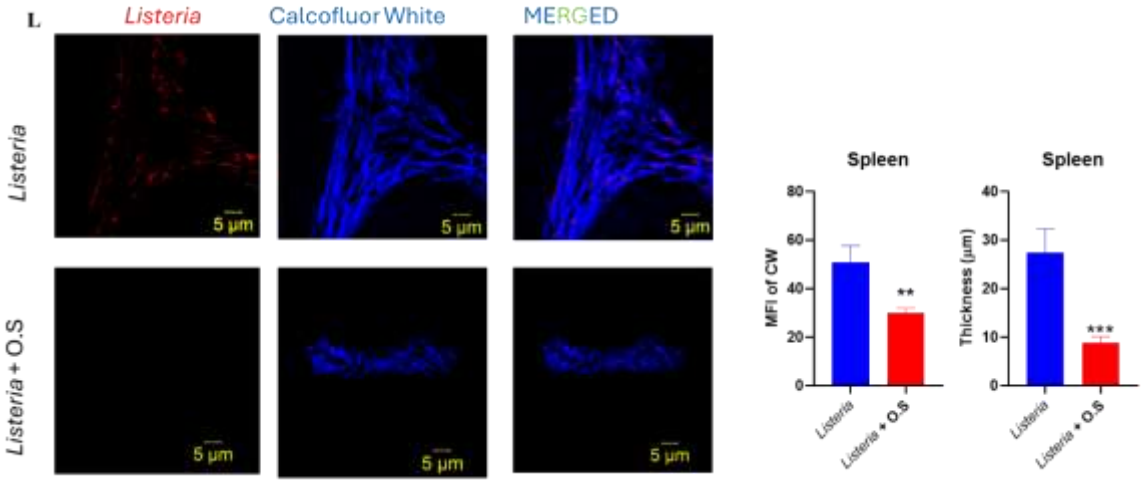
L
Listeria
Calcofluor White
MERGED
Listeria
Listeria + O.S
5 µm
Spleen
MFI of CW
Thickness (µm)
**
***
Listeria
Listeria + O.S

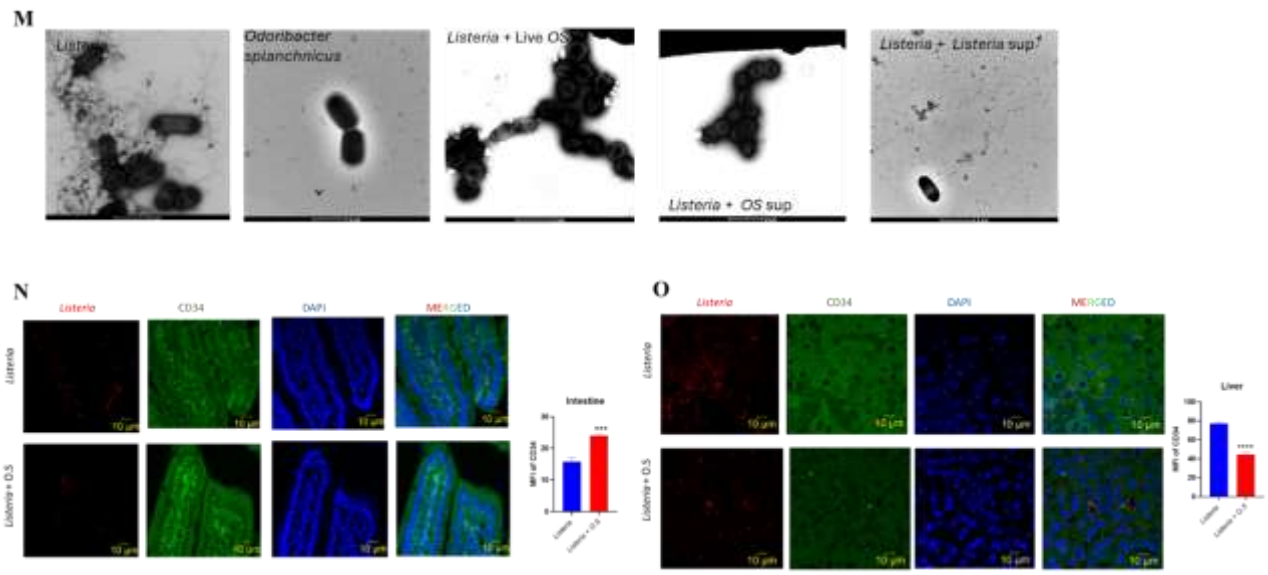

Fig. S3. *Odoribacter splanchnicus* gut colonization protects mice against *Listeria monocytogenes* pathogenesis similar to *Salmonella* infection

A-Haematoxylin-eosin-stained intestinal sections harvested from OS non-colonized or colonized mice cohorts at 5th-day-post-LM-infection. 0-represents normal pathology, 1-represents- mild pathology, 2-3-represents severe pathology.

B-Quantitative gene expression data of several antimicrobial peptides (AMPs) precursor genes in LM-infected mice intestinal tissues harvested at 5th day post-infection from OS colonized or non-colonized cohorts. Unpaired Student's t-test is performed to obtain the p-values. Data is representative of N=2, n=5.

C- Haematoxylin-eosin-stained intestinal sections harvested from OS non-colonized or colonized mice cohorts at 5th-day-post-SF-infection. 0-represents normal pathology, 1-represents- mild pathology, 2-3-represents severe pathology.

D- Quantitative gene expression data of several antimicrobial peptides (AMPs) precursor genes in SF-infected mice intestinal tissues harvested at 5th-dpi from O.S colonized or non-colonized cohorts. Unpaired Student's t-test is performed to obtain the p-values. Data is representative of N=2, n=5.

E- Quantitative gene expression study of tight junction protein genes *Tjp1*, *Claudin5*, GVB damage marker *PV-1*, angiogenesis marker-*Vegf,* and *Axin2* in LM- infected mice intestinal tissues harvested at 5th-dpi from OS colonized or non-colonized cohorts. Unpaired Student's t-test is performed to obtain the p-values. Data is representative of N=2, n=5.

F- Quantitative gene expression study of tight junction protein genes *Tjp1*, *Claudin5*, GVB damage marker *PV-1*, angiogenesis marker-*Vegf,* and *Axin2* in SF-infected mice intestinal tissues harvested at 5th-dpi from OS-colonized or non-colonized cohorts. Unpaired Student's t-test is performed to obtain the p-values. Data is representative of N=2, n=5.

G-H- Intestinal Immunohistochemical sections representing PV-1 protein expression (G) and Muc2 (H) in intestinal tissues of OS-non-colonized and colonized mice cohorts upon LM infection.

I-J- Intestinal Immunohistochemical sections representing PV-1 protein expression (I) and Muc2 (J) in intestinal tissues of OS non-colonized and colonized mice cohorts upon SF infection.

K- Representative Calcofluor white (CW) staining of STM-infected mice spleen tissues at 5th-dpi.

L- Representative CW staining of LM-infected mice spleen tissues at 5th-dpi.

M- Transmission Electron Microscopic (TEM) images of LM in presence or absence of LM supernatant, OS and its supernatant to assess the possession of flagella.

N-O- Immunohistochemical sections representing CD34 (an endothelial marker of vasculature) protein expression in intestinal (N) and liver (O) tissues of OS non-colonized and colonized mice cohorts upon LM infection. Data is representative of N=2, n=3 (tissue samples). Un-paired t-test was used to obtain the p-values.

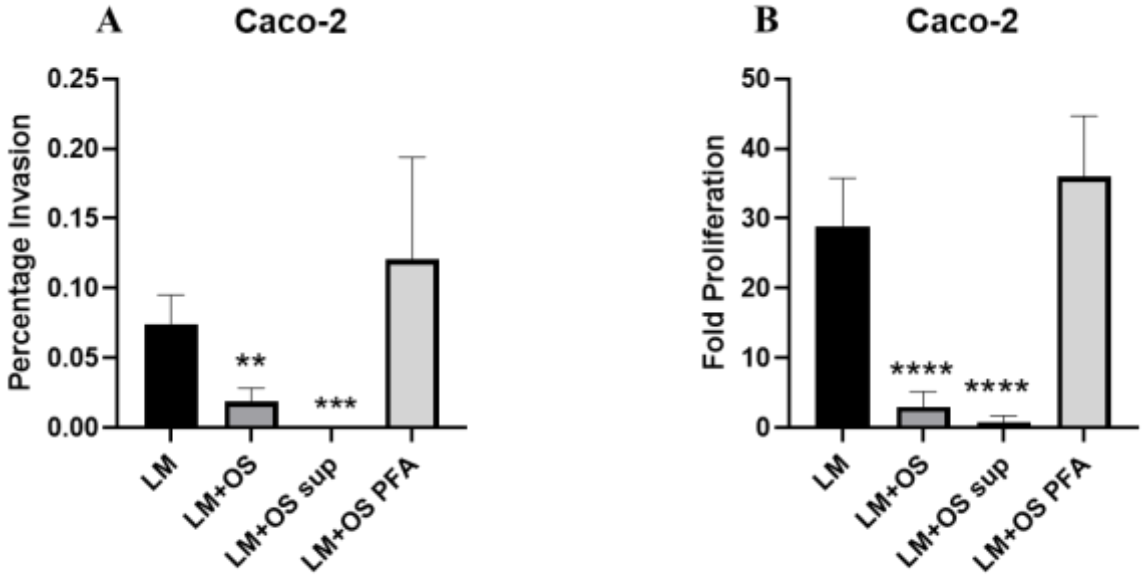

Fig. S4 ***Odoribacter splanchnicus*** **and its culture supernatant restricts** ***Listeria monocytogenes*** **pathogenesis in human intestinal cells**

A- Percent invasion of LM in Caco-2 cells in presence or absence of live OS, OS sup, PFA-fixed-OS. Data is representative of N=3, n=3. Unpaired t-test is used to obtain the p-values.

B-Intracellular fold proliferation of LM in Caco-2 cells in the presence or absence of live OS, OS sup, PFA-fixed-OS. Data is representative of N=3, n=3. Unpaired t-test is used to obtain the p-values.

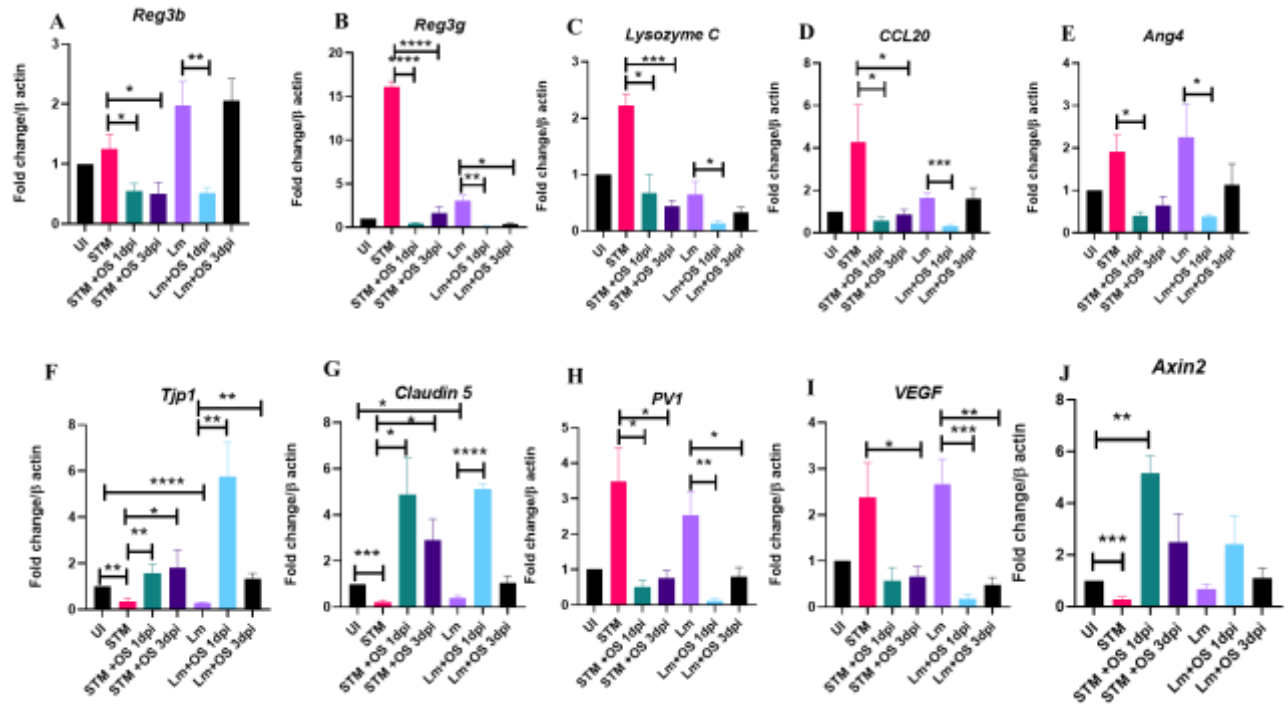
A
Reg3b
B
Reg3g
C
Lysozyme C
D
CCL20
E
Ang4
F
Tjp1
G
Claudin 5
H
PV1
I
VEGF
J
Axin2
Fold change/β actin
UI
STM
STM +OS 1dpi
STM +OS 3dpi
Lm
Lm+OS 1dpi
Lm+OS 3dpi

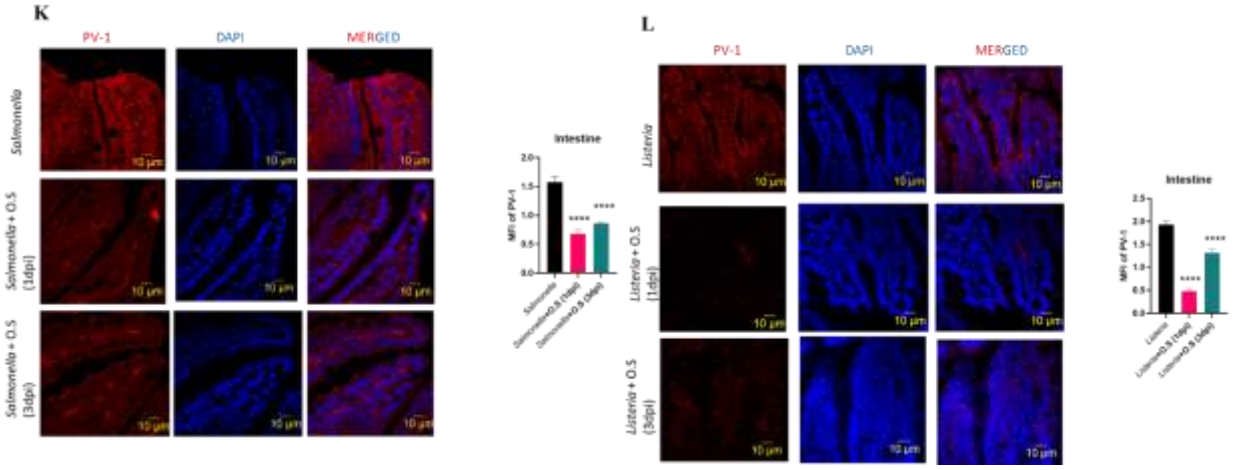
K
PV-1
DAPI
MERGED
Salmonella
Salmonella + O.S (1dpi)
Salmonella + O.S (3dpi)
Intestine
L
Listeria
Listeria + O.S (1dpi)
Listeria + O.S (3dpi)

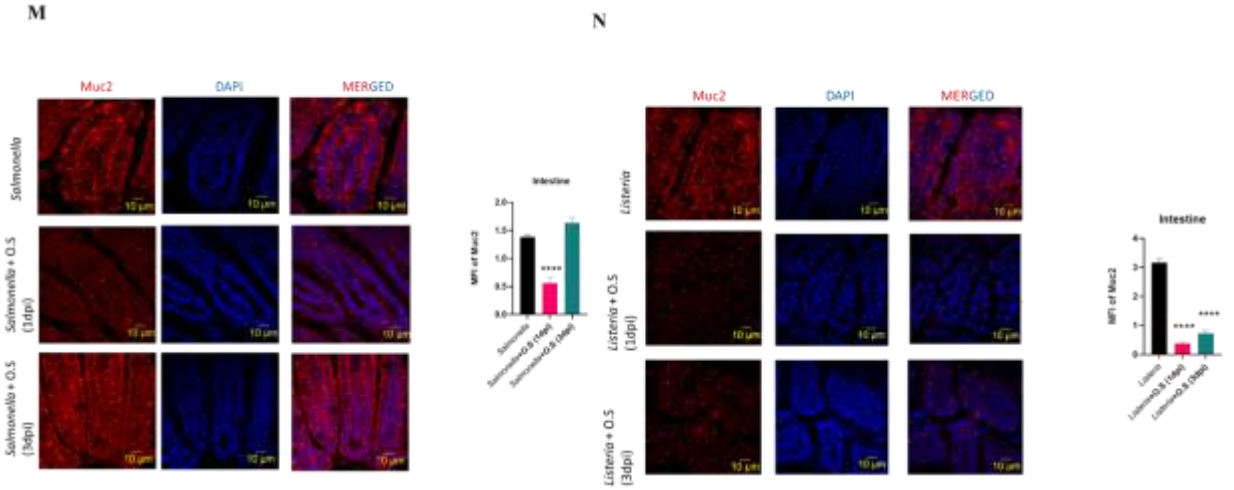
M
Muc2
DAPI
MERGED
Salmonella
Salmonella + O.S (1dpi)
Salmonella + O.S (3dpi)
Intestine
N
Listeria
Listeria + O.S (1dpi)
Listeria + O.S (3dpi)

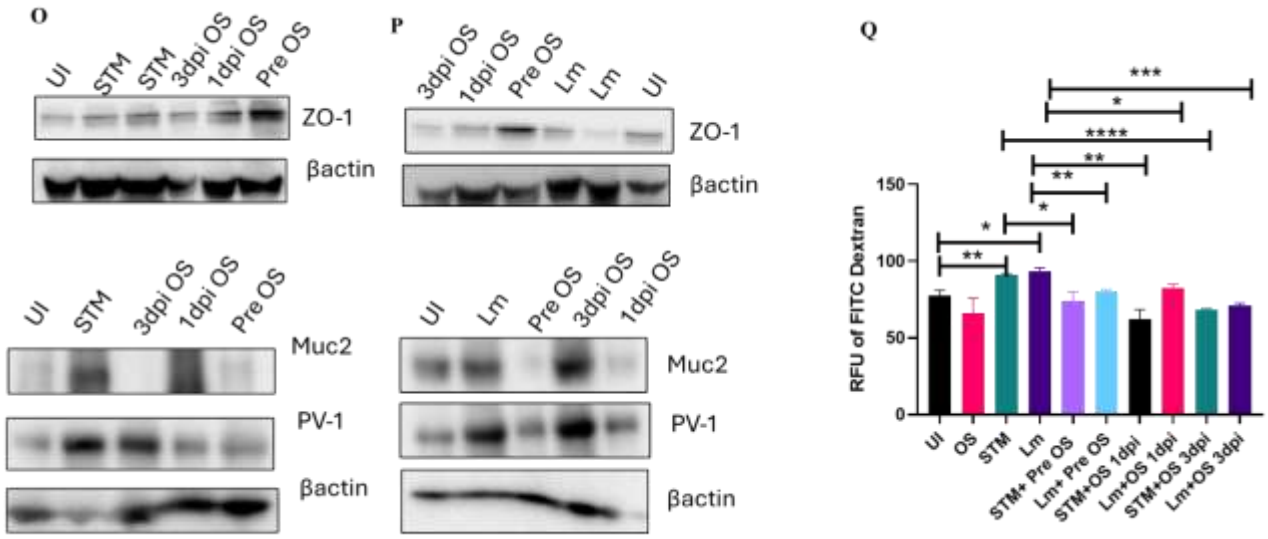

Fig. S5 *Odoribacter splanchnicus* administration post-establishment of infection protected mice against *Listeria monocytogenes* and *Salmonella* Typhimurium

A-E-Quantitative gene expression data of several antimicrobial peptides (AMPs) precursor genes in LM and STM-infected mice intestinal tissues harvested at 5th dpi upon OS colonization at 1-dpi or 3-dpi. Unpaired Student's t-test is performed to obtain the p-values. Data is representative of N=2, n=5.

F-J- Quantitative gene expression study of tight junction protein genes *Tjp1*, *Claudin5*, GVB damage marker *PV-1*, angiogenesis marker-*Vegf,* and *Axin2* in LM and STM-infected mice intestinal tissues harvested at 5th-dpi upon OS colonization at 1-dpi or 3-dpi. Unpaired Student's t-test is performed to obtain the p-values. Data is representative of N=2, n=5.

K-L- Intestinal Immunohistochemical sections representing PV-1 protein expression in *Salmonella* (K) or *Listeria* (L)-infected mice harvested on 5th-dpi with or without OS administration at 1-dpi or 3-dpi.

M-N- Intestinal Immunohistochemical sections representing Muc2 protein expression in *Salmonella* (M) or *Listeria* (N)-infected mice harvested on the 5th dpi with or without OS administration at 1-dpi or 3-dpi.

O-P- Immunoblotting representing the protein expression profile of Muc2, ZO-1, and PV-1 in *Salmonella* (O) or *Listeria* (P)-infected mice intestinal tissue harvested on 5th-dpi with or without OS pre-or post-colonization (1-dpi or 3-dpi).

Q- Estimation of FITC fluorescence in mice plasma via gut permeability assay in *Salmonella* or *Listeria*-infected mice cohorts with or without OS pre-or post-colonization (1dpi or 3dpi) upon oral administration of FITC Dextran (25mg/kg) 4h before euthanization at 5th-dpi.

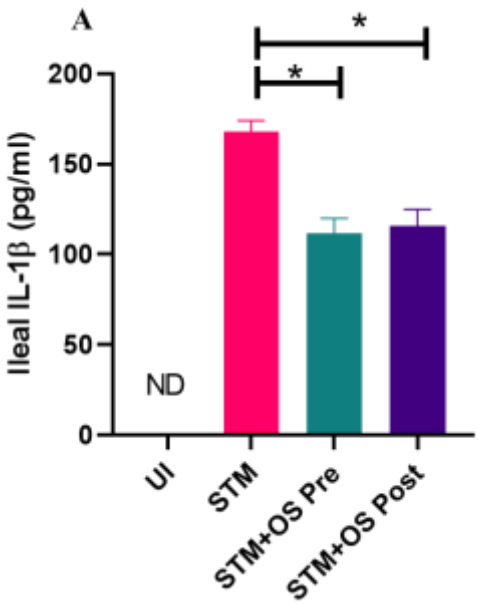

Fig. S6 *Odoribacter splanchnicus* alleviates *Salmonella*-induced intestinal inflammation in mice both during pre and post-treatment

A- Estimation of IL-1β in the ileal sections of UI or *Salmonell*a-infected mice tissues harvested at 5th dpi with or without OS pre-or post-colonization (1dpi).

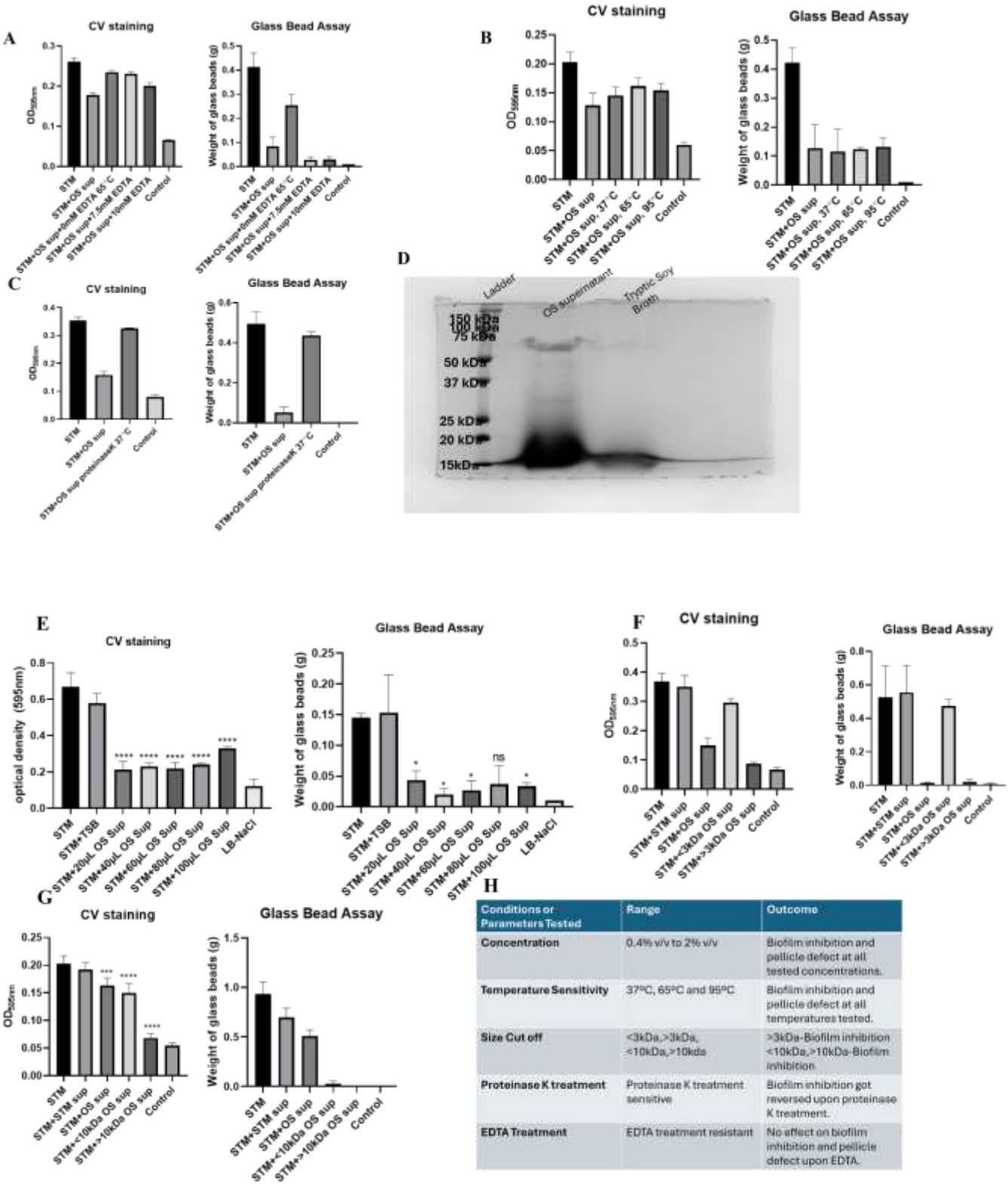

H

Conditions or Parameters Tested	Range	Outcome
Concentration	0.4% v/v to 2% v/v	Biofilm inhibition and pellicle defect at all tested concentrations.
Temperature Sensitivity	37ºC, 65ºC and 95ºC	Biofilm inhibition and pellicle defect at all temperatures tested.
Size Cut off	<3kDa,>3kDa, <10kDa,>10kda	>3kDa-Biofilm inhibition <10kDa,>10kDa-Biofilm inhibition
Proteinase K treatment	Proteinase K treatment sensitive	Biofilm inhibition got reversed upon proteinase K treatment.
EDTA Treatment	EDTA treatment resistant	No effect on biofilm inhibition and pellicle defect upon EDTA.

I Comparison of Gel Filtration fraction peaks of Protein Standard versus Sample

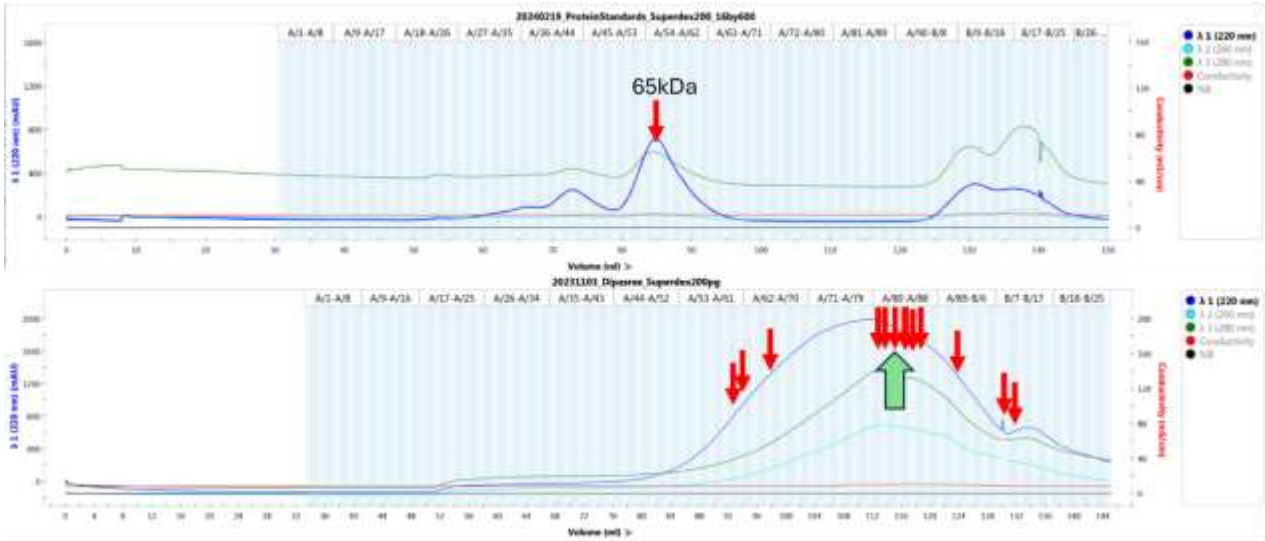

Fractions showing inhibitory effect

Fractions exhibiting highest inhibitory activity upon titration

A82, A83, and A84- Fractions exhibiting highest inhibitory activity upon titration

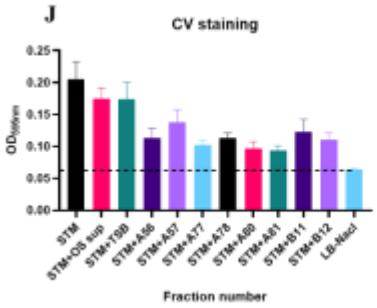

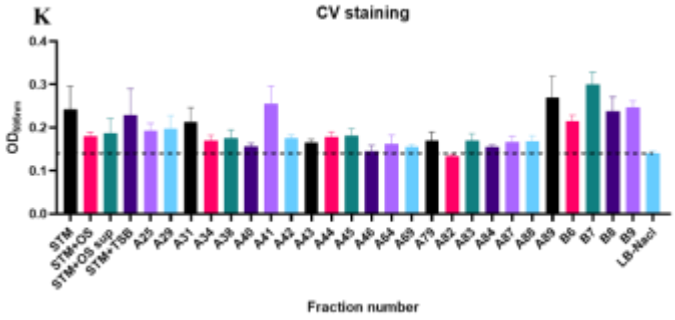

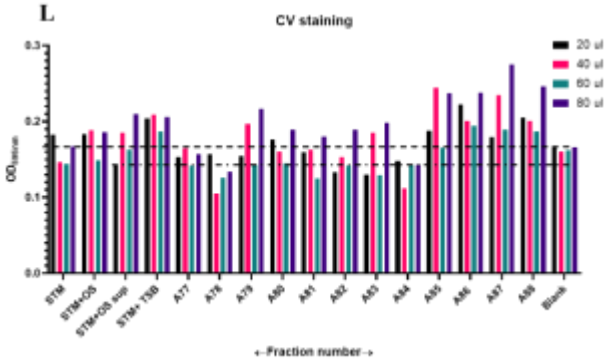

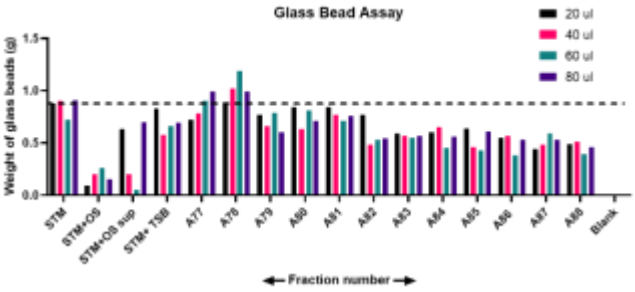

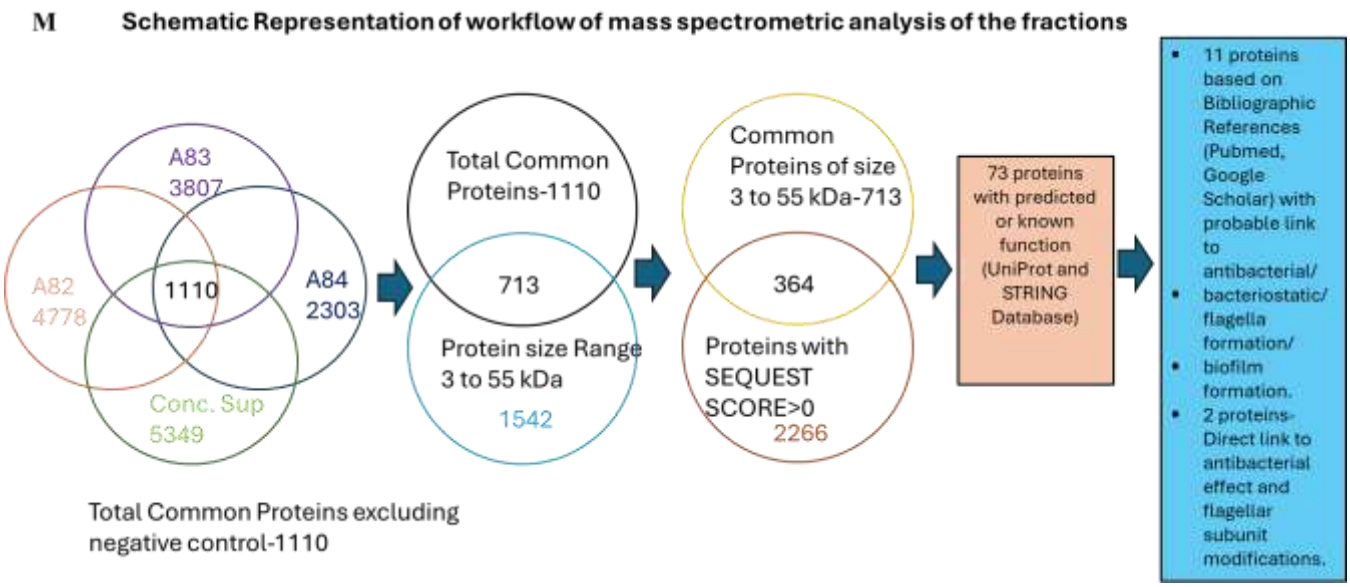

Fig. S7 Characterization of the inhibitory active molecule within *O. splanchnicus* culture supernatant

A- Biofilm assay showing the biofilm formation ability of STM after 72h of inoculation in presence of OS culture supernatant upon EDTA treatment. Data is representative of N=4, n=4. Unpaired t-test is used to obtain the p-values.

B- Biofilm assay showing the biofilm formation ability of STM after 72h of inoculation in presence of OS culture supernatant at high temperature conditions. Data is representative of N=4, n=4. Unpaired t-test is used to obtain the p-values.

C- Biofilm assay showing the biofilm formation ability of STM after 72h of inoculation in presence of OS culture supernatant under Proteinase K treatment. Data is representative of N=4, n=4. Unpaired t-test is used to obtain the p-values.

D- Coomassie-stained SDS-PAGE demonstrating the size range of the differential protein bands present in OS supernatant as opposed to the tryptic soy broth media control.

E- Biofilm assay showing the biofilm formation ability of STM after 72h of inoculation in presence of varying concentration OS culture supernatant. Data is representative of N=4, n=4. Unpaired t-test is used to obtain the p-values.

F- Biofilm assay showing the biofilm formation ability of STM after 72h of inoculation in presence of OS culture supernatant fractions fractionated using 3kDa Amicon filter. Data is representative of N=4, n=4. Unpaired t-test is used to obtain the p-values.

G- Biofilm assay showing the biofilm formation ability of STM after 72h of inoculation in presence of OS culture supernatant fractions fractionated using 10kDa Amicon filter. Data is representative of N=4, n=4. Unpaired t-test is used to obtain the p-values.

H- Summary table demonstrating the conditions tested for active molecule characterization and their effective outcome.

I-Gel filtration chromatogram of protein standards and the OS culture supernatant. Red arrow shows the fractions with biofilm inhibitory activity. Green arrow depict the fraction with highest inhibitory activity.

J-K- Biofilm assay showing the biofilm formation ability of STM after 72h of inoculation in presence of OS supernatant gel filtration fractions. Data is representative of N=2, n=2. Unpaired t-test is used to obtain the p-values.

L- Biofilm assay showing the biofilm formation ability of STM after 72h of inoculation in presence of varying concentration of OS supernatant biofilm inhibitory gel filtration fractions. Data is representative of N=2, n=1. Unpaired t-test is used to obtain the p-values.

M-Schematic representation of the workflow of mass spectrometric analysis of the gel filtration fractions (A82, A83, A84 and Concentrated supernatant).

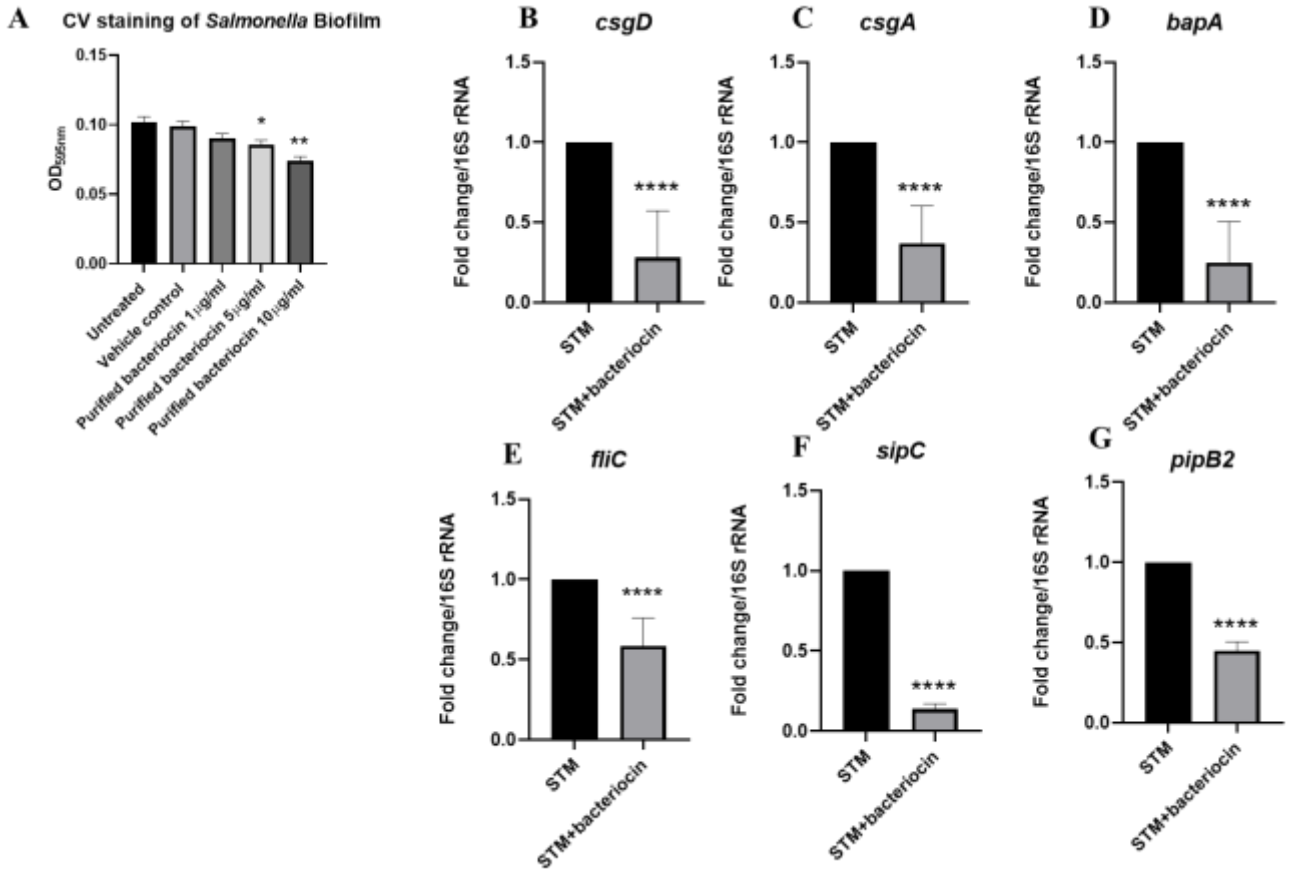

Fig. S8 *O. splanchnicus* bacteriocin attenuates *Salmonella* pathogenesis

A- Biofilm assay showing the biofilm formation ability of STM after 72h of inoculation under varying concentration of OS bacteriocin. Data is representative of N=2, n=2. Unpaired t-test is used to obtain the p-values.

B-G- RT-qPCR mediated gene expression of STM biofilm regulatory genes *csgD* (B), *csgA*(C), *bap* (D), along with flagellar gene *fliC*(E), SPI-1-*sipC* (F) and SPI-2-*pipB2*(G) in presence or absence of OS bacteriocin treatment. Data is representative of N=2, n=5. Unpaired Student's t-test was used to obtain the p-values.

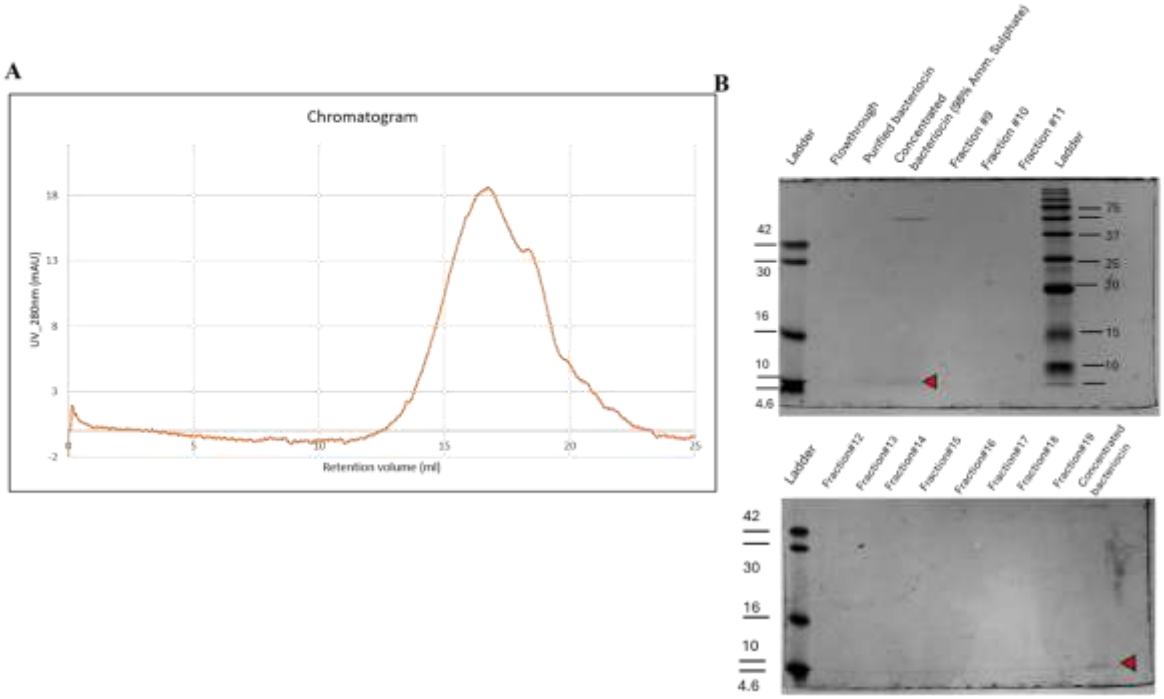

Fig. S9 Purification procedure of *O. splanchnicus* produced bacteriocin via ammonium sulphate precipitation method followed by Fast Performance Liquid Chromatography

A-Size exclusion chromatogram of OS-produced bacteriocin fractions post 95-98% ammonium sulphate precipitation.

B- Coomassie-stained SDS PAGE showing the purified and concentrated OS bacteriocin

Table S1- Selected List of 11 proteins from Mass Spectrometric Analysis based on bibliographic search

Accession ID	Protein Name and	Referenced Function
A0A412WBT8	Immunity protein Imm5 domain-containing protein	Uncharacterized
F9Z8G5	Peptidase	Modulate biofilm formation and host defense.
R6F650	Carboxyl-terminal protease	Critical for post-translational processing and associated with regulation of gene expression, stress response, maintenance of cell envelope integrity and bacterial virulence.
A0A412TJE3	ATP-dependent Clp protease proteolytic subunit	Influence virulence and infectivity of pathogenic bacteria. ClpP enhance biofilm formation in *Enterococcus faecalis*.
F9Z604	Peptidase C39 bacteriocin processing	The cysteine peptidase cleave the double glycine leader peptides from the precursors of bacteriocin
A0A412TJV3	UDP-2,4-diacetamido-2,4, 6-trideoxy-beta-L-altropyranose hydrolase	It catalyzes the third step in the biosynthesis of pseudaminic acid. Pseudaminic acid is a sialic-like sugar that modifies flagellin.
A0A412WSU3	Bacteriocin	Antimicrobial peptides that can kill or inhibit closely related or unrelated bacterial strains.
A0A413I832	Serine Protease	Extracellular proteases regulate biofilm formation and growth of competitors.
A0A412W3J2	Glutamate dehydrogenase	Involved in bacterial response to stress adaptation and virulence.
A0A412WSS0	Bacteriocin	Antimicrobial peptides that can kill or inhibit closely related or unrelated bacterial strains.
F9ZBU9	Peptidylprolyl isomerase	Promote biofilm formation in *Mycobacterium tuberculosis*.

Table S2-List of primers

Primer Name	**Sequence (5'---3')**
O. splanchnicus 16S rRNA FP	ATGTAATGATGAGCACTCTAACGG
O. splanchnicus 16S rRNA RP	GGCTTTTGAGATTGGCATCC
PV-1 FP	CGAACTGGAGGCGCGTAA
PV-1 RP	GCAGCGACTTGGCCTTGAC
Claudin5 FP	CCCAGTTAAGGCACGGGTAG
Claudin5 RP	GGCACCGTCGGATCATAGAA
βactin FP	CAGCAAGCAGGAGTACGATG
βactin RP	GCAGCTCAGTAACAGTCCG
Vegf FP	GCAGCGACAAGGCAGACTAT

Vegf RP	AACCTCCTCAAACCGTTGGC
Tjp1 FP	TCTTGCAAAGTATCCCTTCTGT
Tjp1 RP	CAGAAATCGTGCTGATGTGCC
Reg3b FP	GCTTGTCAAGAGCTTCTGGATTTC
Reg3b RP	TGTCCCTTGTCCATGATGCTC
Reg3g FP	CGCTGAAGCTTCCTTCCTGT
Reg3g RP	GGGTTCATAGCCCAGTGTCG
Lysozyme C FP	GGTCTACAATCGTTGTGAGTTG
Lysozyme C RP	TGAGCTAAACACACCCAGTCA
CCL 20 FP	GCAACTACGACTGTTGCCTC
CCL20 RP	TTCTTGACTCTTAGGCTGAGGA
Ang4 FP	TGGTTGTGATTCCTCCAACTCT
Ang4 RP	TGTTGACATCTTTGCAAGGCG
fliC FP	CTAAACAAACTGGGTGGCGC
fliC RP	GCACCCAGGTCAGAACGTAA
bapA FP	ACGGTGACTACGCCTAAAAC
bapA RP	CTTCCGCCTCAGTCACTTTT
csgD FP	ACGATTATCCCTACCGTGAA
csgD RP	GCGGACTCGGTGCTGTTGTA
Salmonella 16S rRNA FP	GTGAGGTAACGGCTCACCAA
Salmonella 16S rRNA RP	TAACCGCAACACCTTCCTCC
sipC FP	GCAGTACGCCGCTACTCAGG
sipC RP	AGCGCGAATATTGCCTGCGA
pipB2 FP	TGGCGCCAATTTACAACACGC

pipB2 RP	CTCGCCTTTCGCAGGTTTGC

Table S3-List of Antibodies

Antibody Name	**Catalogue Number**
PV-1	A15906-20ul (Abclonal)
CD34	A19015-20ul (Abclonal)
Muc2	A4767 (Abclonal)
ZO-1	R26.4C DHSB
β actin	A3854 (Sigma)
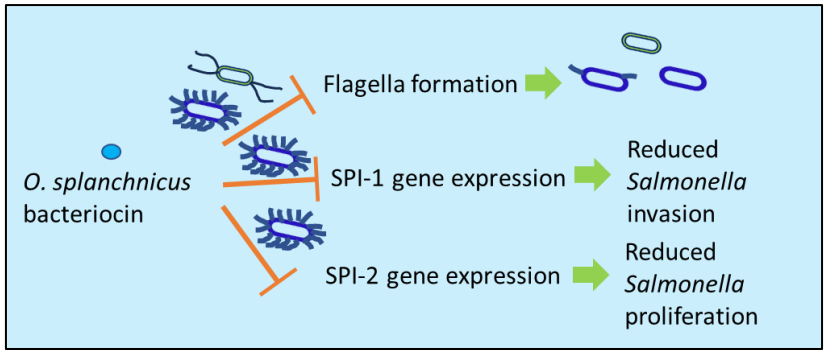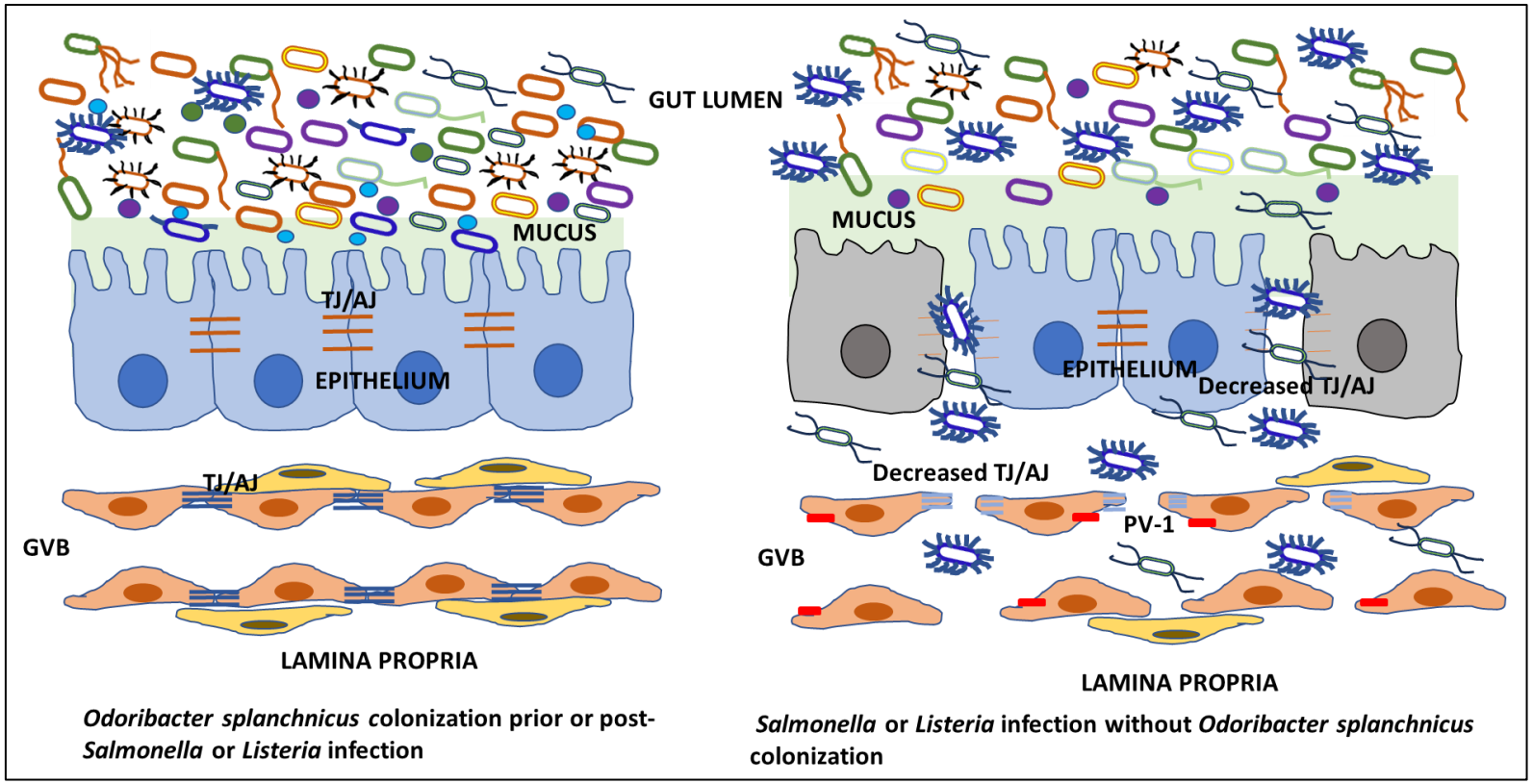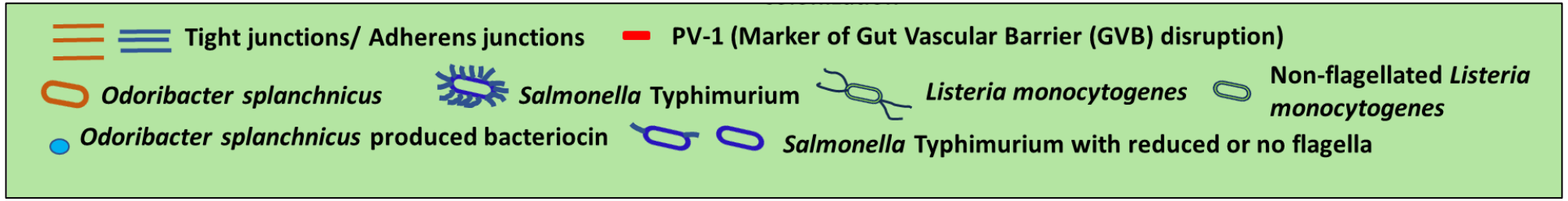
GRAPHICAL ABSTRACT